Clim Dyn
DOI 10.1007/s00382-006-0187-8

Past and future changes in climate and hydrological indicators in the US Northeast

Katharine Hayhoe · Cameron P. Wake · Thomas G. Huntington · Lifeng Luo · Mark D. Schwartz · Justin Sheffield · Eric Wood · Bruce Anderson · James Bradbury · Art DeGaetano · Tara J. Troy · David Wolfe

Received: 22 February 2006 / Accepted: 1 August 2006

Abstract To assess the influence of global climate change at the regional scale, we examine past and future changes in key climate, hydrological, and biophysical indicators across the US Northeast (NE). We first consider the extent to which simulations of twentieth century climate from nine atmosphere-ocean general circulation models (AOGCMs) are able to reproduce observed changes in these indicators. We then evaluate projected future trends in primary climate characteristics and indicators of change, including seasonal temperatures, rainfall and drought, snow cover, soil moisture, streamflow, and changes in biometeorological indicators that depend on threshold or accumulated temperatures such as growing season, frost days, and Spring Indices (SI). Changes in indicators for which temperature-related signals have already been observed (seasonal warming patterns, advances in high-spring streamflow, decreases in snow depth, extended growing seasons, earlier bloom dates) are generally reproduced by past model simulations and are projected to continue in the future. Other indicators for which trends have not yet been observed also show projected future changes consistent with a warmer climate (shrinking snow cover, more frequent droughts, and extended low-flow periods in summer). The magnitude of temperature-driven trends in the future are generally projected to be higher under the Special Report on Emission Scenarios (SRES) mid-high (A2) and higher (A1FI) emissions scenarios than under the lower (B1) scenario. These results provide confidence regarding the direction of many regional climate trends, and highlight the fundamental role of future emissions in determining the potential magnitude of changes we can expect over the coming century.

K. Hayhoe (✉)
Department of Geosciences, Texas Tech University,
Lubbock, TX, USA
e-mail: katharine.hayhoe@ttu.edu

C. P. Wake
Institute for the Study of Earth, Oceans, and Space,
University of New Hampshire, Durham, NH, USA

T. G. Huntington
US Geological Survey, Augusta, ME, USA

L. Luo · J. Sheffield · E. Wood · T. J. Troy
Department of Civil and Environmental Engineering,
Princeton University, Princeton, NJ, USA

M. D. Schwartz
Department of Geography,
University of Wisconsin-Milwaukee,
Milwaukee, WI, USA

B. Anderson
Department of Geography and Environment,
Boston University, Boston, MA, USA

J. Bradbury
Department of Geosciences,
Climate System Research Center,
University of Massachusetts,
Amherst, MA, USA

A. DeGaetano
Northeast Regional Climate Center,
Department of Earth and Atmospheric Sciences,
Cornell University, Ithaca, NY, USA

D. Wolfe
Department of Horticulture,
Cornell University, Ithaca, NY, USA

1 Introduction

Investigating current and future climate change at the regional scale is essential to understanding potential impacts on humans and the natural environment. Atmospheric circulation, topography, land use, and other regional features modify global changes to produce unique patterns of change at the regional scale. As global- and regional-scale changes influence existing natural and human systems, a set of impacts and responses distinctive to each region are produced. For example, the effects of global sea-level rise in regions with steep rocky shorelines would be very different from those for low-lying coastal areas. Global-scale changes may also trigger region-specific feedbacks—temperature increases at higher latitudes could drive snow-albedo feedbacks, with a potential enhancement of local warming, while a similar increase at lower latitudes might increase atmospheric water content and cloudiness, which could moderate such a warming.

Here, we assess the implications of global climate change for the US Northeast (NE), an area encompassing the states of Maine, New Hampshire, Vermont, Massachusetts, Rhode Island, Connecticut, New York, New Jersey, and Pennsylvania. Since 1970, this region has seen increases in temperature of 0.25°C/decade and changes in other related indicators consistent with a warming climate. The number of days that exceed the 95th percentile threshold for daily maximum temperature at northeastern US stations has increased by nearly 1.7 occurrences per decade over the last 45 years (DeGaetano and Allen 2002). Warm minimum temperature extremes (i.e., nights that remain above the daily 95th percentile) have increased at almost double this rate (2.9 occurrences per decade) and more than twice the rate observed in other regions of the US. Extremely cold temperature days also have decreased since 1960, although they have typically decreased at a rate of less than one occurrence per decade (DeGaetano and Allen 2002).

Warming temperatures have also affected the ratio of snow to total precipitation (S/P), and the amount and density of snow on the ground. The S/P ratio decreased at 11 of 21 United States Historical Climatology Network (USHCN) sites in New England from 1948 through 2000 (Huntington et al. 2004). The four sites in northernmost New England with the strongest and most coherent trends showed an average decrease in annual S/P ratio from about 30% in 1949 to 23% in 2000. Huntington et al. (2004) also reported decreasing snowfall amounts at most of the 21 USHCN sites over this period. Furthermore, 18 of 23 snow course sites in Maine with records spanning at least 50 years through 2004 had decreases in snowpack depth or increases in snow density (Hodgkins and Dudley 2006a). Finally, four sites with the longest (1926–2004) and most complete records indicate an average decrease in March/April snowpack depth of 16% and an 11% increase in snow density. Together, these changes in the S/P ratio, snowfall amounts, and snow density/depth combine to present a consistent picture of changes in winter snow driven by warmer temperatures.

Reductions in the length of the ice cover on lakes and rivers has also been observed. These changes are again consistent with warmer air temperatures in late winter and early spring. Records of spring ice-out on lakes in the NE between 1850 and 2000 indicate an advancement of 9 days for lakes in northern and mountainous regions and 16 days for lakes in more southerly regions (Hodgkins et al. 2002). Similarly, historical stream flow records indicate an advance in the timing of high river flows during the twentieth century over the northern part of the NE, where snowmelt dominates the annual hydrological cycle (Hodgkins et al. 2003; Hodgkins and Dudley 2006a). Most of the observed change occurred during the period 1970 through 2000—when winters in the NE were warming at ~0.7°C/decade—with the dates of high flow advancing by 7–14 days (Hodgkins et al. 2003).

Biological responses to climate change have also been detected in the NE. A comprehensive analysis of historical records from 72 sites across the NE, where the first flower date for the same clone of lilac has been monitored since the 1960s, shows an advance of 4 days (Wolfe et al. 2005). The same study also examined first flower data from 1960 to 2000 for grape and apple trees in NY only, and found an advance of 6–8 days for these woody perennials. Using herbarium specimens at the Harvard University Arnold Arboretum (Cambridge, MA, USA), Primack et al. (2004) found that flowering was occurring on average 8 days earlier from 1980 to 2002 than it did from 1900 to 1920.

In addition to plant responses, changes in fauna have also been observed. For example, Gibbs and Breisch (2001) documented an advance of 10–13 days in first date of spring mating calls in upstate NY since the beginning of the century, for four of six frog species studied. Advances in the timing of migration of anadromous fish (Atlantic salmon and alewives) in NE rivers during the last few decades have also been recently reported (Huntington et al. 2003; Juanes et al. 2004).

These and other trends suggest that the impacts of climate change are already being experienced across the NE. Furthermore, most of the changes observed to date are consistent with what would be expected from a warming trend. As global temperatures continue to rise over the next century driven by human emissions of greenhouse gases, how will these and other indicators of regional change in the NE be affected? In each of the following sections, we address this question in two steps. First, we examine the extent to which historical model simulations that incorporate both natural variability and human drivers of climate change are able to reproduce trends in surface climate, hydrology, and biometeorological indicators over the past century. Then, we assess future model-simulated trends in these key climate indicators and interpret these trends in the context of past changes, in order to assess the potential direction and magnitude of future change under higher and lower emission scenarios.

2 Data sources and methods

2.1 Observational data sources

The observational data used in this analysis are a subset of the USHCN instrumental temperature and precipitation records (Karl et al. 1990; Easterling et al. 1999; Williams et al. 2005). These represent the best available data for investigating changes since 1900, as the stations were selected based on length and quality of data, which includes limiting the number of station changes. In addition, monthly data have undergone numerous quality assurances and adjustments to best characterize the actual variability in climate. These adjustments take into consideration the validity of extreme outliers, time of observation bias (Karl et al. 1986), changes in instrumentation (Quayle et al. 1991), random relocations of stations (Karl and Williams 1987), and urban warming biases (Karl et al. 1988). Missing data are estimated from surrounding stations to produce a nearly continuous data set for each station.

Annual and seasonal temperature and precipitation trends for the entire region were calculated using the monthly USHCN data as follows. First, the mean for all station data in each of the National Climatic Data Center climate divisions (Guttman and Quayle 1996) was calculated based on monthly temperature and precipitation data, with typically less than six stations per division. Then, the area-weighted regional mean of the climate division data was calculated, representing the data from 73 stations for the temperature analysis and 93 stations for the precipitation analysis. No weight was given to climate divisions with no stations; however, these only represent 6% of the total area of the study region for the temperature analysis, and 11% for the precipitation analysis. Daily USHCN data were used as input to the freeze date analysis and the Spring Indices (SI) models.

In addition to the surface data, sea surface temperature reconstructions for the historical period were derived for the Gulf of Maine and the Gulf Stream in the southern part of the NE based on the NOAA Extended Reconstructed sea-surface temperature (SST) data (Smith and Reynolds 2003), was provided by the NOAA-CIRES Climate Diagnostics Center[1].

2.2 Climate models and emission scenarios for future projections

The model analysis presented here is based on output from nine of the latest coupled atmosphere-ocean general circulation models (AOGCMs) available from the IPCC AR4 WG1 database, as listed in Table 1. Historical model simulations (1900–1999) correspond to the CMIP ''Twentieth Century Climate in Coupled Models'' or 20C3M scenarios. These represent each modeling group's best efforts to reproduce observed climate over the past century. As such, they can include forcing from anthropogenic emissions of greenhouse gases, aerosols, and reactive species; changes in solar output; particulate emissions from volcanic eruptions; changes in tropospheric and stratospheric ozone; and other influences required to provide a comprehensive picture of climate over the last century.

It is important to note, however, that although the 20C3M simulations are all intended to represent the same historical total-forcing scenarios (including both natural variability as well as the effect of human emissions on climate), due to the uncertainty in estimating changes in natural and human-related forcings over the last century, they do not necessarily have identical boundary conditions. Some inter-model differences as well as discrepencies between model simulations and observations, therefore, may also be a result of differing input conditions.

Future AOGCM simulations (2000–2099) are all forced using the same IPCC Special Report on Emission Scenarios (SRES, Nakićenović et al. 2000) higher (A1FI), mid-high (A2), and lower (B1) emissions scenarios. These scenarios use projections of changes in population, demographics, technology, international trade, and other socio-economic factors

[1] http://www.cdc.noaa.gov/

Table 1 Key characteristics of the nine atmosphere-ocean general circulation models (AOGCMs) and their output used in this analysis

Model acronym	Host institution	SRES scenarios	Resolution		References
			Atmospheric	Oceanic	
CCSM3	NCAR (USA)	A2, B1	1.4° × 1.4°	0.46° × 1.125°	Collins et al. (2006)
CGCM3	CCCMA (Canada)	A2, B1	3.75° × 3.75°	1.875° × 1.875°	Kim et al. (2002, 2003)
CSIRO Mk3	ABM (Australia)	A2, B1	1.875° × 1.875°	0.95° × 1.875°	Gordon et al. (2002)
GFDL CM2.1	NOAA/GFDL (USA)	A1FI, A2, B1	2° × 2.5°	0.9° × 1.0°	Delworth et al. (2006)
GISS E-R	NASA/GISS (USA)	A2, B1	4° × 5°	4° × 5°	Schmidt et al. (2006)
HadCM3	UKMO (UK)	A1FI, A2, B1	2.5° × 3.75°	1.25° × 1.25°	Pope et al. (2000)
ECHAM5	MPI (Germany)	A2, B1	1.875° × 1.875°	1.0° × 1.0°	Roeckner et al. (2003)
MIROC-med	CCSR (Japan)	A2, B1	2.81° × 2.81°	0.9° × 1.4°	Hasumi and Emori (2004)
PCM	NCAR (USA)	A1FI, A2, B1	2.81° × 2.81°	1.0° × 1.0°	Washington et al. (2000)

All models have 17 atmospheric levels unless indicated otherwise

to estimate corresponding emissions of greenhouse gases and other radiatively active species. Although the SRES scenarios do not include any explicit policies aimed at reducing greenhouse gas emissions to mitigate climate change, the B1 scenario can be seen as proxy for stabilizing atmospheric CO_2 concentrations at or above 550 ppm, as levels reach this value by 2100. Atmospheric CO_2 concentrations for the higher A1FI scenario are 970 ppm by 2100 and 830 ppm for A2. Information from these scenarios used to drive the future AOGCM simulations include regional changes in emissions of greenhouse gases and reactive species. Although changes in land use and hence vegetation cover are implicit in these emissions estimates, feedbacks between emissions and climate are not included in the AOGCM simulations used here.

The broader analyses of monthly temperature and precipitation presented here are based on results from the full set of nine AOGCMs and multiple ensemble members, as summarized in Table 1. At the time of this analysis, only two models (HadCM3 and PCM) had produced daily output for both A1FI and B1 simulations. As the higher A1FI and lower B1 scenarios are expected to show the largest difference between projected impacts (Hayhoe et al. 2004), our intensive hydrological analysis focuses primarily on the A1FI and B1 simulations from these two models. A1FI output from a third model, GFDL, recently became available and these projections have been added to the broader analysis. Further analyses of changes in sea surface temperatures and biometeorological indices were limited by the availability of monthly ocean output (available for only five of nine models: CCSM, CGCM3, HadCM3, Miroc, and PCM) and daily temperature output (available for the periods 2046–2065 and 2081–2099 only for four of nine models: CGCM3, CSIRO, ECHAM5, and Miroc).

2.3 Hydrological modeling

For the hydrological modeling, monthly AOGCM temperature and precipitation fields were first statistically downscaled to daily values with a resolution of 1/8°, after Wood et al. (2002). This downscaling used an empirical statistical technique that maps the probability density functions for modeled monthly and daily precipitation and temperature for the climatological period (1961–1990) onto those of gridded historical observed data. In this way, the mean and variability of both monthly and daily observations are reproduced by the climate model output. The bias correction and spatial disaggregation technique is one originally developed for adjusting AOGCM output for long-range streamflow forecasting (Wood et al. 2002), later adapted for use in studies examining the hydrologic impacts of climate change (VanRheenan et al. 2004).

This method compares favorably to other statistical and dynamic downscaling techniques (Wood et al. 2004). It also carries the additional benefit of being able to generate the daily climate inputs required to drive the hydrological model for models and scenarios that did not save their output at daily resolution (e.g., HadCM3 A1FI; also true for A2 and B1 simulations from CGCM3, CSIRO, ECHAM5, and Miroc). However, there are also some disadvantages to this approach. First, statistical generation of daily values from monthly temperature and precipitation means that these do not reflect possible changes in atmospheric circulation as simulated by the global models on scales of days to weeks, except so far as these

are reflected by the global models' monthly means. Furthermore, this approach assumes that the shapes (although not the mean) of the monthly historical temperature and precipitation distributions used to generate the daily values for each month remain unchanged over time. This assumption may not be valid for many regions of the globe, where model-simulated increases in daily extremes are often not directly proportional to what would be projected based on shifts in the mean value alone (e.g., Wehner 2004). For that reason, K. Hayhoe et al. (personal communication) compared the performance of this statistical downscaling (SD) method for the NE with available dynamic regional model simulations (RCM) driven by the PCM model. Overall, we found the two methods to be relatively comparable for this region. For most of the temperature range, SD-based estimates of changes in the distribution were within 5% of RCM-generated estimates (except between ~28 and 33°C, where the SD frequencies were higher). Projected precipitation changes by the SD and RCM methods were generally within 5% of each other as well, except for relatively small precipitation events of <10 mm/day, where SD projected a decrease but RCM output, an increase.

Downscaled temperature and precipitation were then used as input to the Variable Infiltration Capacity (VIC) model (Liang et al. 1994, 1996; Cherkauer et al. 2002). This hydrological model simulates the full water and energy balance at the earth's surface by modeling processes such as canopy interception, evapotranspiration, runoff generation, infiltration, soil water drainage, and snow pack accumulation and melt. Model forcings (precipitation, temperature, radiation, etc.), soil properties (porosity, saturated hydraulic conductivity, etc.) and vegetation parameters (leaf area index, stomatal and architectural resistances, etc.) are specified at each grid cell.

Outputs from the VIC model include gridded fields of evapotranspiration, runoff, snow water equivalent (SWE) and soil moisture profiles. The runoff fields (surface and baseflow) from these simulations are then routed through stream networks using a lumped routing model (for small basins) that can be compared with observed streamflow measurements for the historical period of the record.

The VIC model has been applied extensively at scales ranging from river basin (Abdulla et al. 1996), regional and continental (Maurer et al. 2002), up to global scales (Nijssen et al. 2001; Sheffield et al. 2004a). Applications of the VIC model to the continental US include two retrospective simulations driven by observed precipitation and temperature, combined with NCEP reanalysis wind fields and predictive relationships for vapor pressure, incoming long-wave and short-wave radiation, and air pressure. The first was for the period 1950–1999 at 1/8° resolution (Maurer et al. 2002) and the second from 1915 to 2003 at 0.5° resolution (Hamlet and Lettenmaier 2005). These simulations compare well with observations of soil moisture and other hydrologic variables (Maurer et al. 2001, 2002), and form the basis of the analysis of historical land surface hydrology presented here.

Here we expand on Maurer et al. (2001, 2002) to compare the retrospective (observation-based) VIC simulations with available observations for the NE, consisting of observed USGS streamflow measurements from a number of small, unregulated basins scattered across the region. The basins are generally located in headwaters of more remote regions and do not suffer from human influences such as reservoir storage and water abstractions. The VIC model can simulate observed streamflow reasonably well, with correlations between model-simulated and observed streamflow ranging from 0.6 to 0.9 except for winter streamflow toward the northern half of the domain (Fig. 1). Underestimation of peak streamflow in higher elevation regions during the winter may be due in part to underestimation of precipitation because of the tendency for rain gauges to be located in valley bottoms. The VIC model also appears to capture the magnitude and seasonal cycle of streamflow at the monthly time scale.

For this study, a set of four climate simulations were also run, using downscaled precipitation and temperature from the PCM and HadCM3 20C3M (past) and A1FI and B1 (future) simulations for the period 1960–2099. It is assumed that the relationship between (although not the actual values of) monthly temperature and precipitation and the sub-monthly forcing statistics such as rain day frequency, ratio of snow/rain, and number of freezing days remains unchanged in the future period. Although this does allow sub-monthly statistics to shift with the mean of the distribution, the assumption of no change in the shape of the distribution, particularly in the tails where extreme events occur, is likely to be conservative based on both historical observations (Huntington et al. 2004) as well as future projections (K. Hayhoe et al., personal communication). Potential changes in climate forcings such as diurnal temperature range (DTR), radiation, and cloud cover, as well as external forcings such as vegetation (including the lengthening of the growing season) and land use, are not accounted for in these simulations. This means that the explicit influence of climate change on DTR, temperature or precipitation

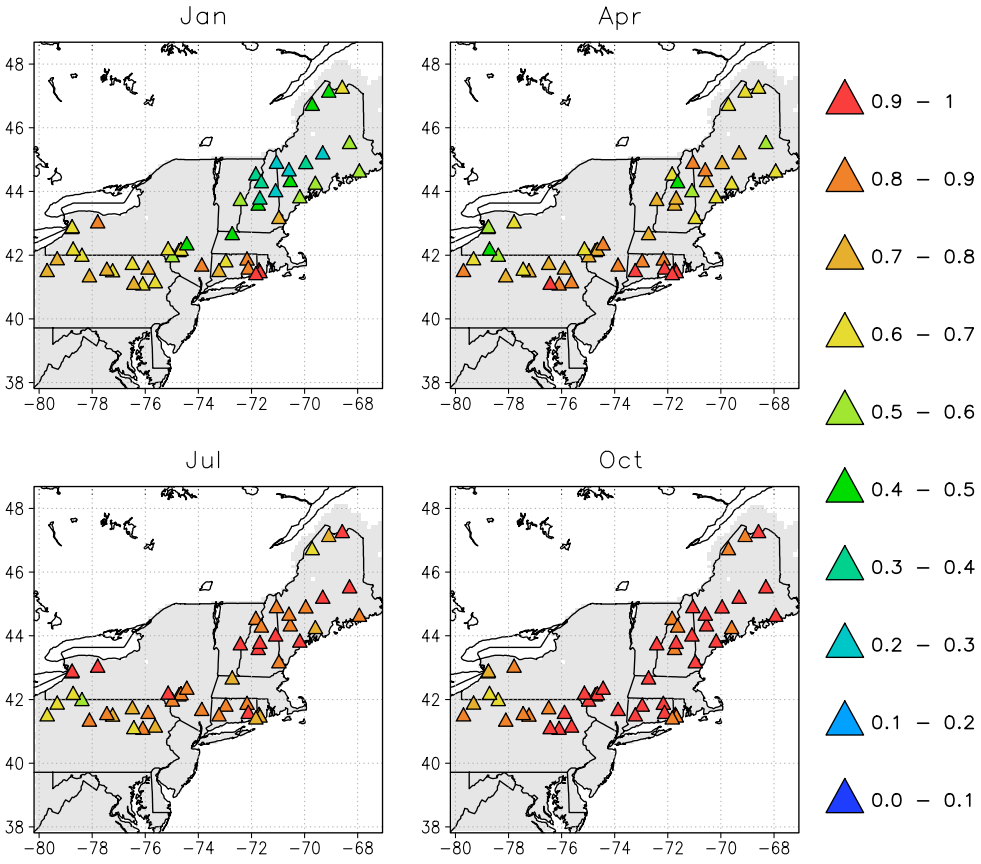

Fig. 1 Correlation between observed monthly gauge-based streamflow amounts and VIC-simulated monthly streamflow for a 50-year (1950–1999) retrospective simulation driven by observed historical temperature and precipitation. *Triangles* indicate locations of selected-unregulated basins for which correlations were calculated. A correlation of 1 indicates a perfect match between observed and model-simulated monthly anomalies, while lower values quantify the strength of the correlation at that location

variance, transpiration fluxes from the extended growing season, and other daily climatological metrics will not be represented by VIC outputs. In this sense, the VIC downscaled climate projections are a direct representation of inter-monthly AOGCM forcing, coupled with terrain-related adjustments based on the Parameter-elevation Regressions on Independent Slopes Model (PRISM, Daly et al. 1997) to resolve finer-scale topographical features.

2.4 Spring Indices models

The SI models (Schwartz 1997; Schwartz and Reiter 2000) were developed from over 2,000 station-years of weather data combined with first leaf and first bloom data for lilac, and to a lesser degree, honeysuckle. These data were collected from 1961 to 1994 at sites throughout the north-central and northeastern USA. The SI models are a set of linked multiple regression-based models developed to simulate the spring phenology of three regionally important species: cloned lilac (Syringa chinensis ''Red Rothomagensis'') and cloned honeysuckle (Lonicera tatarica ''Arnold Red'' and L. korolkowii ''Zabeli''). Model simulations of first-leaf and first-bloom dates are based on the number of high degree-days accumulated. They are also affected by synoptic weather events that occur after winter chilling requirements (i.e., vernalization) has been satisfied, particularly events that occur within about 1 week of first leaf. Species-specific values are first calculated, then averaged to produce composite output for three component models: chilling date (when the required winter rest condition has been satisfied), first leaf date (indicative of initial understory plant growth, when the land surface becomes ''active'' in energy exchange), and first bloom date (indicative of overstory plant growth), as described in Schwartz (1997). The SI models have been extensively tested and shown to be representative of the general development of mid-latitude forest trees and shrubs that are temperature-responsive and not water-limited in spring (Schwartz et al. 2006). These models and associated suite of measures (including last spring frost date, first autumn frost date, and related values) can be calculated for any sets of daily T_{max}/T_{min}, given the latitude of the station (Schwartz and Reiter 2000). Here, they have been calculated based on gridded downscaled historical and future simulated changes in NE

temperatures. This produces a ''pooled'' analysis for the entire NE region starting in 1916 and extending out to 2099. First leaf and first bloom dates were calculated for individual grid points, which were then averaged to provide a regional average date for first leaf and bloom.

3 Basic climate indicators

Changes in annual and seasonal temperature and precipitation serve as primary indicators of climate change. These also drive changes in hydrological and biological indicators. Hence, we first examine observed and historical simulated temperature and precipitation trends across the NE. We then assess future changes in temperature and precipitation that may occur under higher and lower emission scenarios as projected by a range of AOGCMs with varying degrees of sensitivity. This analysis places future temperature and precipitation changes in the context of what has already been observed across the region. It also qualifies the amount of uncertainty in regional projections that is due to our understanding of the climate system (as represented by the temperature change projected to occur by multiple models under a single emissions scenario) as compared with the uncertainty due to projections of socio-economic and other types of human development over such long time scales (represented by the temperature changes projected to occur under different emissions scenarios).

3.1 Temperature

Annual temperatures over the NE have risen an average of +0.08 ± 0.01°C/decade over the last century. This rate has increased significantly over the recent three decades to a rate of +0.25 ± 0.01°C/decade. The greatest changes over the last 35 years have been seen in winter, which has warmed at 0.70 ± 0.05°C/decade, almost a degree per decade (see also Keim et al. 2003; Trombulak and Wolfson 2004). On average, observed annual temperatures in the 1990s were 0.6°C warmer than the 1900–1999 long-term mean. In the 1990s, temperatures were also greater in winter (1.1°C) than summer (0.4°C) relative to the long-term mean.

In comparing observed trends with historical model simulations, an important clarification must be made. The AOGCM simulations used here are not constrained by prescribed sea surface temperatures or other boundary conditions that would force them to match observed year-to-year climate variations. Hence, there is no reason per se to expect an AOGCM to reproduce the specific timing of a warm or cold year, or even a trend over shorter period of time that would be dominated by the natural variability of the climate system. Furthermore, the sensitivity of linear trends to the end-points of the time series used to calculate such a trend suggest that even over a 30-year period, differences in the timing of natural climate fluctuations are likely to result in at least some differences in the magnitude of model-simulated versus observed trends that should not be taken as indicative of the models' ability to reproduce long-term climate trends.

Despite these caveats, most models are able to reproduce 100-year and even the 30-year trend in annual temperature over the NE, with a model ensemble average trend from 1900 to 1999 of +0.08 ± 0.06°C/decade and a higher trend of +0.23 ± 0.11°C/decade from 1970 to 1999, as compared with observed trends of +0.08 ± 0.01 and 0.25±0.01°C/decade, respectively (Table 2). This suggests: first, that external forcings rather than internal variability may be responsible for the greater part of the observed trend; and second, that most AOGCMs are able to translate external forcing into regional temperature trends of the correct sign but tend to under-estimate the correct magnitude of recent change.

Long-term (1900–1999) AOGCM ensemble average seasonal temperatures are also similar to observed, although with higher variability. Winter (DJF) modelled temperature trends are +0.12 ± 0.16°C/decade, as compared with observed trends of +0.12 ± 0.02°C/decade, while summer (JJA) modelled trends are 0.07 ± 0.06°C/decade as compared with 0.07 ± 0.01°C/decade observed. From 1970 to 2000, however, models do not appear to capture the seasonal trends well, significantly under-estimating them in winter and over-estimating them in summer. Over the short-term, observed winter temperatures increased at a rate of +0.7 ± 0.05°C/decade, while the AOGCM ensemble average increase was only +0.25 ± 0.26°C/decade. The observed summer trend was +0.12 ± 0.02°C/decade, while modeled trends averaged +0.29 ± 0.14°C/decade. This suggests that the models are not able to capture the regional and/or larger-scale characteristics that have enhanced observed winter warming over the last few decades. In fact, indications are that AOGCMs tend to under-estimate the magnitude of both past and recent observed change over the NE. Dynamical features may be producing the model winter biases, such as a failure to resolve the changing albedo due to snow loss.

In the future, temperatures across the NE are projected to continue to increase. Greater increases (significant at the 0.001 level) are seen under higher A1FI

Table 2 Comparison of observed with multi-model ensemble average simulated trends in primary climate indicators for the NE over the past century (length of record) and the last three decades (1970–2000)

	Units	Period of record		1970–2000	
		OBS	MOD	OBS	MOD
Temperature (1900–1999)					
Annual	°C/decade	+0.08	+0.08	+0.25	+0.23
Winter (DJF)	°C/decade	+0.12	+0.12	+0.70	+0.25
Summer (JJA)	°C/decade	+0.07	+0.07	+0.12	+0.29
Precipitation (1900–1999)					
Annual	mm/decade	+10	+0.7	–8	+7
Winter (DJF)	mm/decade	–0.5	+0.5	+3	+3
Summer (JJA)	mm/decade	+1	–0.3	–0.2	+0.6
Sea surface temperatures (1900–2000)					
Gulf of Maine	°C/decade	+0.5	+0.8	+0.06	+0.6
Gulf Stream	°C/decade	+0.3	+0.4	–0.20	+0.3
Terrestrial hydrology[a,b] (1950–1999)					
Evaporation	mm/day/decade	+0.014	+0.006	–0.027	–0.040
Runoff	mm/day/decade	+0.032	+0.022	–0.017	–0.015
Soil moisture	%sat/decade	+0.005	+0.023	–0.0014	–0.0029
Streamflow[b] (1950–1999)					
Timing of spring peak flow centroid	days/decade	–0.44	+0.27	–0.21	–0.11
7-day low-flow amount	%/decade	+2.8	–0.25	–1.77	+0.22
Snow[a,b] (1950–1999)					
Total SWE	mm/decade	–0.025	+0.05	–3.52	–2.90
Number of snow days	days/month/decade	–0.040	–0.07	–0.52	–0.60
Spring indices (1916–2003)					
First leaf	days/decade	–0.44	–0.05	–2.19	–1.39
First bloom	days/decade	–0.41	–0.20	–0.92	–0.69

[a] "Observed" estimates of long- and short-term trends in region-wide average evaporation, runoff, soil moisture and SWE are based on the retrospective VIC simulation driven by observed temperature and precipitation, while "modeled" estimates are based on VIC simulations driven by HadCM3 and PCM 20C3M simulations

[b] Modeled trends for period of record are from 1960 to 1999 only. Observed trends are shown for length of record starting in 1950 to avoid beginning linear trends near the 1960s drought

and A2 scenarios relative to the lower B1 scenario in all seasons by end-of-century, and for summer and annually by 2035–2064. Projected increases in annual regional surface temperature average 5.3°C by 2070–2099 relative to 1961–1990 under A1FI[2] and 4.5°C increase under A2 as compared with 2.9°C under B1 (Fig. 2; Table 3). Toward end-of-century, models also project an equal or larger increase in summer as compared with winter temperatures (Table 3). As this is in contrast to the greater trend in winter temperatures that has been observed to date, we speculate that it may be related to regional-scale feedbacks in the water balance connected to both a decrease in the relative importance of the snow-albedo feedbacks (as overall snow cover decreases) as well as summer drying and enhanced warming due to increased evaporation.

These temperature increases have the potential to impact a range of meteorological events and other climate indicators across the NE. One of the more obvious impacts to be expected is on temperature extremes. As mean temperature increases, the distribution of daily temperatures shifts toward the warmer end of the spectrum, increasing the number of days that fall above the present-day high-temperature thresholds for warm temperatures and decreasing the days that fall below cold-temperature thresholds (DeGaetano and Allen 2002). Regional model simulations for the NE (K. Hayhoe et al., personal communication) show 20–40 more days per year above the 1990 90th percentile threshold by the 2090s under the A1FI scenario, while Diffenbaugh et al. (2005) estimated increases of 30–40 days/year in the NE in the 95th percentile by late-twenty-first century under A2. This represents an approximately twofold increase in the occurrence rate, highlighting the potential for both changes in mean seasonal temperatures as well as future shifts in the climatological daily temperature distribution.

3.2 Precipitation

In addition to temperature, precipitation is an important aspect of climate in the NE. However, inter-annual

[2] Based on available A1FI simulations from HadCM3, GFDL CM2.1 and PCM1 only.

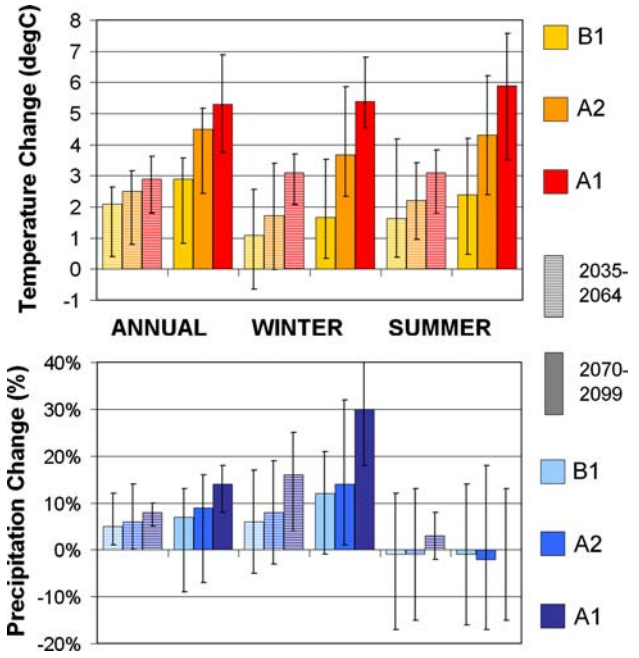

Fig. 2 Projected changes in annual, winter (*DJF*) and summer (*JJA*) temperature (°C) and precipitation (%) under the SRES B1 (*low*), A2 (*mid-high*) and A1FI (*higher*) emissions scenarios for the periods 2035–2064 and 2070–2099 relative to the 1961–1990 average over the US Northeast. *Solid bars* indicate the ensemble average value from 9 AOGCMs (B1, A2) and 3 AOGCMs (A1FI), while the whiskers indicate the range of projections from individual simulations. All models consistently indicate increases in temperature over all seasons and in annual and winter precipitation that become greater over time. They also indicate a larger temperature change under higher relative to lower emissions scenarios

variability in precipitation is generally much higher than that of temperature. This makes it more difficult to distinguish consistent long-term trends from natural fluctuations. In particular, historical records are dominated by the 1960s drought, a multi-year event estimated to be the most severe drought to occur in that region in the observational record (Leathers et al. 2000). As the AOGCM simulations are unconstrained by observations, these may simulate droughts of a similar magnitude (as examined later in this analysis) but not necessarily at the same time. Hence, care must be used in estimating long-term precipitation trends, as any trends that begin or end near a major drought event (or a extended wet period) will be biased by this very strong event.

Despite uncertainty in determining long-term trends, historical records do show a consistent long-term trend in annual precipitation of +9.5 ± 2 mm/decade over the last century (as also found by Keim et al. 2005). These changes are split between spring, summer and fall, with seasonal trends of +2.4 ± 0.3 mm/decade for spring and fall, 1.2 ± 0.5 mm/decade for summer, but little change (–0.5 ± 1 mm/decade) in winter. Since 1970, there is some indication of a reversal of the seasonal trends seen over the previous century. Annually, there is a decrease of –8 ± 9 mm/decade, with a decrease in spring and fall (–2 ± 3 mm/decade), little change in summer, and a slight increase of +3 ± 3 mm/decade in winter precipitation. However, given the sensitivity of precipitation trends to the length of the period used to determine the trend and the large interdecadal variability in precipitation characteristic of the NE, these trends are not robust.

A range of positive and negative trends result from AOGCM simulations, with an average annual trend of +0.7 ± 3 mm/decade over the last century, and +7 ± 18 mm/decade from 1970 to 2000. With the sole exception of winter precipitation from 1970 to 2000 (+3 mm/decade for both observed and model average), modeled changes in seasonal precipitation do not match observed, although the high variability associated with model-based trends certainly encompasses the observed trends. This suggests that the observed trend in precipitation in the NE at least over the last century may be primarily driven by natural variability rather than a long-term climate trend.

Regarding the recently observed and model-simulated increase in winter precipitation, however, future projections from almost all model simulations show consistent increases in winter precipitation and no change to a decrease in summer rainfall. Specifically, by end-of-century, winter precipitation is projected to increase an average of 11% under B1 and 14% under A2, but show small decreases (on the order of a few percent) in summer precipitation (Fig. 2, Table 3). These trends are in agreement with what has been observed in the recent past, suggesting there may be a global climate change-related signal in seasonal precipitation that is beginning to emerge from the observational record but is not yet evident in model simulations. These winter precipitation increases are also dynamically consistent with a projected westward shift in the seasonal mean position of the East Coast trough in some of the models (J. Bradbury, personal communication).

Increases in winter precipitation and no change or decreases in summer rainfall will also alter the mean distribution of precipitation in the NE. Increases in heavy precipitation (greater than 2 in. in less than 48 h) have already been observed across much of the NE, particularly during the 1980s and 1990s relative to earlier in the century (Wake and Markham 2005). Further increases are expected in many locations around the world, including the NE (Wehner 2004; Tebaldi et al. 2006). This is generally consistent with

Table 3 Absolute values for the reference period 1961–1990 and projected future changes in key climate indicators for the period 2035–2064 and 2070–2099

	Units	1961–1990	2035–2064			2070–2099		
		20C3M	B1	A2	A1F1	B1	A2	A1FI
Temperature								
Annual	°C	7.8	**+2.1**	**+2.5**	**±2.9**	**+2.9**	**±4.5**	**±5.3**
Winter (DJF)	°C	–4.8	+1.1	+1.7	**+3.1**	+**1.7**	**±3.7**	**±5.4**
Summer (JJA)	°C	20.0	**+1.6**	**+2.2**	**±3.1**	+**2.4**	**±4.3**	**±5.9**
Precipitation								
Annual	cm (%)	102.9	+5%	+6%	**+8%**	+7%	**+9%**	**+14%**
Winter (DJF)	cm (%)	20.95	+6%	+8%	**+16%**	+12%	+14%	**+30%**
Summer (JJA)	cm (%)	28.03	–1%	–1%	+3%	–1%	–2%	0%
Sea surface temperatures[a]								
Gulf of Maine	°C	11.6[a]	+1.3[a]	+1.5[b]	–	**+1.9**[a]	**±3.3**[b]	–
Gulf Stream	°C	23.4[a]	+0.9[a]	**+1.3**[b]	–	**+1.2**[a]	**±2.3**[b]	–
Terrestrial hydrology								
Evaporation	mm/day	1.80	+0.10	–	+0.16	**+0.16**	–	**+0.20**
Runoff	mm/day	1.14	+0.12	–	+0.09	**+0.21**	–	+0.18
Soil moisture	%sat	55.0	+0.4	–	+0.02	+1.0	–	–0.07
Streamflow								
Timing of spring peak flow centroid	days	84.5	–5	–	–8	**–11**	–	**–13**
Low flow days (Q < 0.0367 $m^3/s/km^2$)	days	65.5	–14	–	–1.5	–26	–	+22
7-day low-flow amount	%	100	–4	–	–1	–4	–	**–11**
Drought frequency								
Short	no. of droughts per 30 years	12.61	+5.12	–	+7.19	+3.06	–	**±9.99**
Medium	no. of droughts per 30 years	0.57	+0.03	–	+0.51	+0.39	–	**±2.21**
Long	no. of droughts per 30 years	0.03	+0.03	–	+0.11	+0.04	–	**±0.39**
Snow								
Total SWE	mm	11.0	–4.4	–	**–5.5**	**–5.9**	–	**–9.3**
Number of snow days	days/month	5.2	**–1.7**	–	**–2.2**	**–2.4**	–	**–3.8**
Growing season[b]								
First frost (autumn)	day	295	+1	**±16**	–	**+6**	**±20**	–
Last frost (spring)	day	111	–8	**–14**	–	**–16**	**–23**	–
Length of growing season	days	184	**+12**	**±27**	–	**±29**	**±43**	–
Spring indices[b]								
First leaf	day	98.8	**–3.0**	**–5.2**	**–3.9**	**–6.7**	**–15**	**–15**
First bloom	day	128.8	**–3.7**	**–6.0**	**–5.6**	**–6.3**	**–15**	**–16**

Changes significantly different relative to the 1961–1990 annual distribution at the 99.9% confidence level or higher as determined by a Student's t-test are highlighted in **bold**, and changes significantly different under A1FI and/or A2 relative to B1 at the 99.9% confidence level are underlined

[a]Based on SST output (''tos'') from HadCM3, MIROC, CGCM CCSM, and PCM only

[b]Time periods restricted by output availability to 2047–2065 and 2082–2099

observed historical trends toward an intensification of the hydrologic cycle (Huntington 2006).

Precipitation clearly impacts both human and natural systems throughout the NE. Due to the large interannual variability and uncertainty in estimated trends, more weight should be attached to temperature-driven changes than precipitation. However, given the consistency between the sign of the seasonal trends in observations over the last few decades and future model simulations, we also consider in the following analyses the impact of increasing winter precipitation on snow cover and spring streamflow, and of no change or a decrease in summer rainfall on summer drying and drought.

3.3 Sea surface temperatures

The final basic climate indicator examined here is regional sea surface temperatures (SSTs). SSTs are an important boundary condition on NE climate, as they determine the steepness of the north-to-south air temperature gradient across the region. Variability in regional SSTs has also been linked to surface climate anomalies in the NE, including the 1960s drought (Namias 1966; Bradbury et al. 2002). Off-shore, baroclinicity and storm tracking can respond themodynamically to SST anomalies in the vicinity of the steep meridional SST gradient at the northern boundary of the Gulf Stream, creating positive feedback cycles

(Kushnir et al. 2002) that may affect atmospheric instability over the NE region on seasonal or longer time-scales.

Over the past century, a trend of +0.5°C/decade has been observed in regional SSTs in the Gulf of Maine and +0.3°C/decade in the Gulf Stream region (Fig. 3), with similar but slightly larger trends (+0.8°C/decade and +0.4°C/decade, respectively), being simulated by five of nine AOGCMs examined here for which ocean surface temperature outputs were available[3]. As shown in Fig. 3, the models are generally able to capture the seasonal cycles in terms of the average monthly means and the variance. The models are particularly skillful in the vicinity of the Gulf Stream, east of Cape Hatteras. However, the CCSM3, HadCM3, and MIROC models display a warm bias in the northern Gulf of Maine coastal region, where SSTs are largely influenced by the southeasterly Labrador Current. CGCM3 and PCM do not appear to have these biases in the north and, thus, more realistically simulate the steep SST gradient observed at the northern boundary of the Gulf Stream. This may be indicative of a general problem with the ability of global models to capture the complex ocean currents in this part of the Atlantic, such as the Labrador Current. Other more detailed studies (e.g., Dai et al. 2004) have shown that PCM also displays a systematic warm bias in ocean temperatures, which is at least partially due to its resolution, as it fails to resolve the smaller-scale processes and topographic features that determine the latitude at which the Gulf Stream separates from the eastern coast of North America.

In the future, regional SSTs are projected to increase in accordance with regional air temperatures (Table 3), with larger and more consistent year-round changes under the higher forcing scenario. By 2070–2099, the annually averaged steep SST gradient north of the Gulf Stream is projected to decrease by 15–20%, continuing the trends already seen in both observations and AOGCM simulations of the twentieth century. This implies potential impacts on NE surface climate, as feedbacks between SST anomalies and atmospheric instability may weaken. These temperature increases also have the potential to directly impact temperature-sensitive marine species that live in the waters, for example expanding the range of warm water species northward and permitting invasive species to expand into previously colder waters.

[3] Monthly SST outputs for the historical and future periods were available from the CCSM3, CGCM3, HadCM3, Miroc (med res) and PCM1 models.

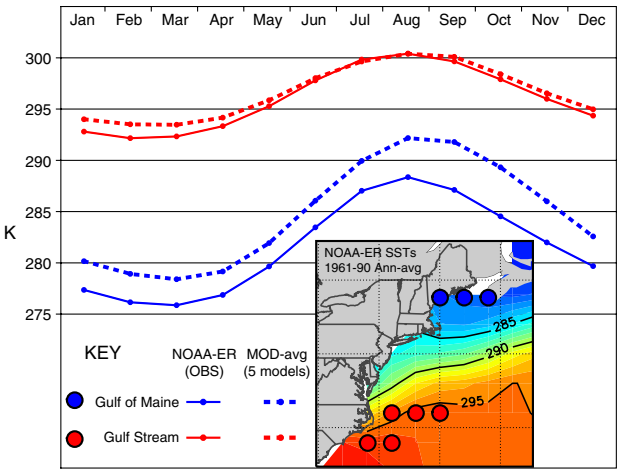

Fig. 3 Comparison of the seasonal cycle in observed mean sea surface temperatures (1961–1990) for the Gulf of Maine and a southern Gulf Stream region with 5-model average SSTs. Inset figure shows grid-points from the NOAA-ER SST dataset—color coded with respect to the line graphs—on which regional averages were based, with comparable grids used for each model, and observed annual average SSTs, in degrees Kelvin

4 Hydrological indicators

Changes in NE hydrology are driven by both temperature and precipitation. In terms of temperature, we have already seen historical advances in the dates of spring ice-out on lakes across the NE and in the timing of high-river flows over the northern part of the domain that are positively correlated with late winter/early spring surface air temperatures (Hodgkins et al. 2003). In addition, precipitation affects the total amount of water available as contributions to streamflow, groundwater, and lake levels, and the timing of peak and low flows as well as extreme events. Here, we examine four types of hydrological indicators that would be expected to affect natural and human systems across the NE: terrestrial hydrological indicators (evaporation, soil moisture, and runoff), summer drying or drought, streamflow, and winter snow cover.

4.1 Evaporation, soil moisture, and runoff

Observations are insufficient to determine long-term and spatially coherent trends in most terrestrial hydrological variables across the NE. For that reason, we assess historical climatological averages and trends in regionally-averaged water balance components from the 50-year retrospective VIC simulation driven by observed temperature and precipitation records.

Similar to precipitation, the time series of major components of the hydrological cycle in the NE are

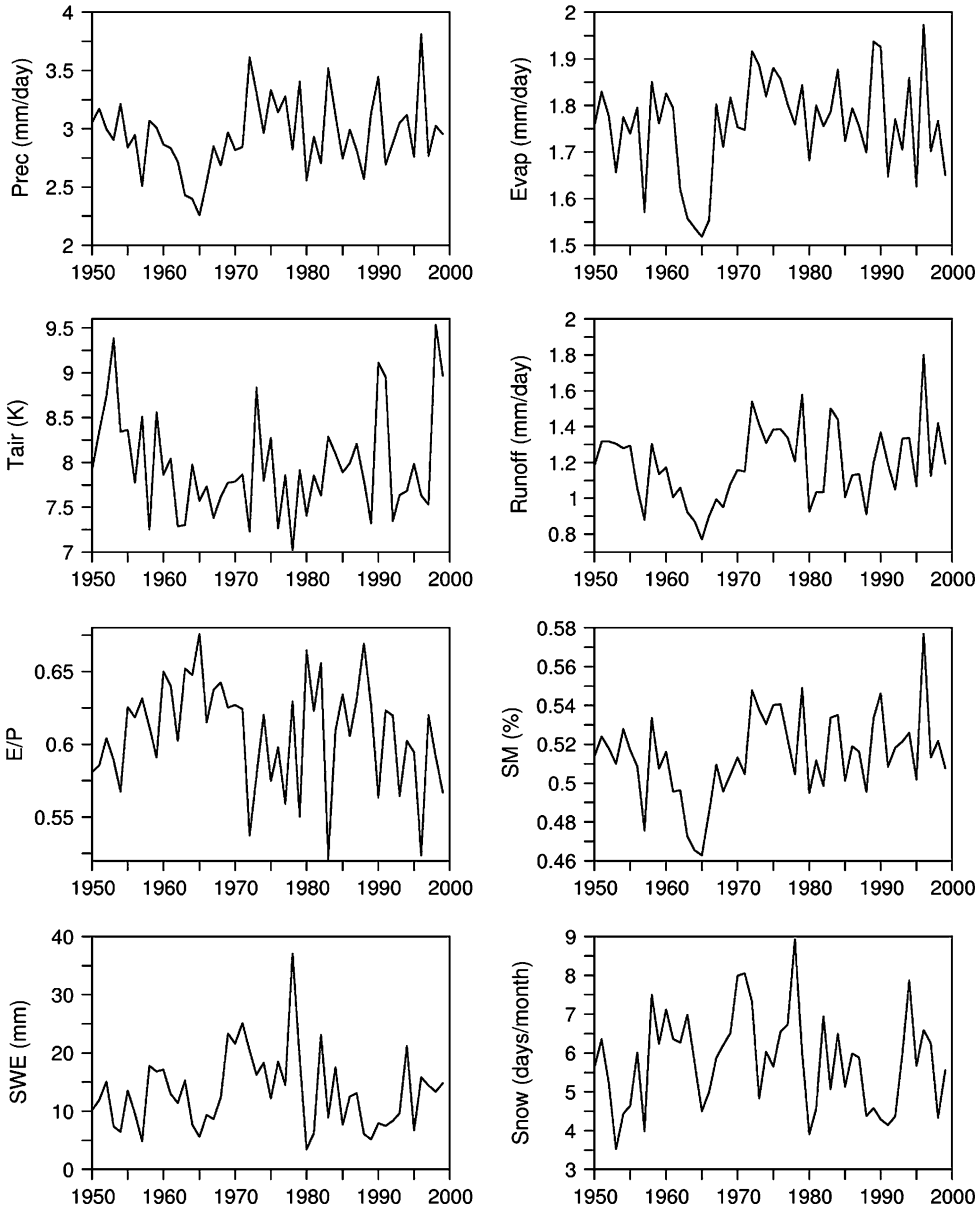

Fig. 4 Annual time series of regionally averaged air temperature, precipitation, and water balance components (evaporation-to-precipitation ratio, snow water equivalent, runoff, soil moisture, and snow cover) from the 50-year retrospective VIC simulation driven by observed temperature and precipitation records from 1950 to 1999. The signature of the 1960s drought is seen in the time series of precipitation, evaporation, runoff, and soil moisture

dominated by the drought period in the mid-1960s (Namias 1966). This event resulted in the lowest values of evaporation, runoff ,and soil moisture seen over the last 50 years (Fig. 4). A non-parametric test of trends from 1950 to 2000 indicates slight increases in evapotranspiration, runoff and soil moisture (weighted by the 1960s drought at the beginning of the period), although none of these changes are statistically significant (Table 2). The last 30 years (1970–1999) show decreasing, but also not significant, trends in water balance components that are generally consistent with increasing temperatures and little change in rainfall over that time. AOGCM-driven VIC simulations for the 20C3M scenario show trends of the same sign over both time periods.

Over the coming century, projected wetter winters and warmer temperatures drive increases in winter runoff, decreases in spring runoff, and increases in annual runoff as peak runoff shifts to earlier in the year (Fig. 5; Table 3). Changes in runoff are generally greater under the higher A1FI scenario as compared with the lower B1, and for the more sensitive HadCM3 model as compared with the less sensitive PCM. Regionally, changes in precipitation and hence runoff are most pronounced in the north. For example, in the southwest part of the domain (region 1, PA–NY),

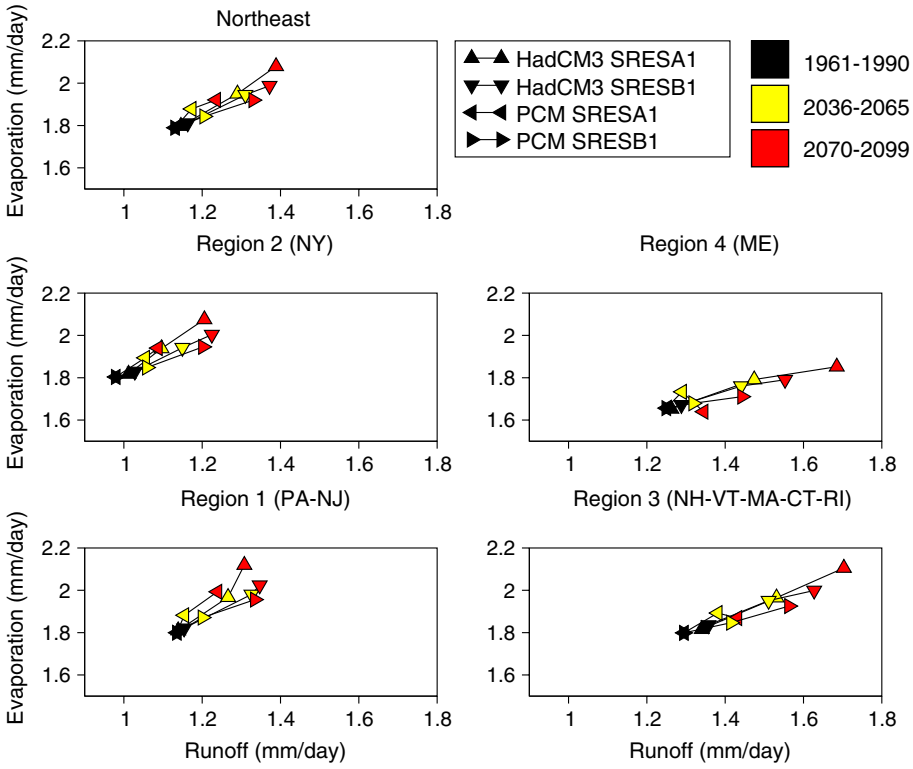

Fig. 5 30-year mean annual evapotranspiration versus runoff from the four future climate simulations (HadCM3 and PCM A1FI and B1) averaged over the NE region and the four sub-regions. Both evaporation and runoff tend to increase over time, with proportionally greater increases in runoff relative to evaporation in regions 3 and 4 as compared with regions 1 and 2

increases in runoff range from 9 to 18% as compared with 11–27% in the northeast (region 3, NH–VT–MA–CT–RI).

Rising temperatures are projected to increase evaporation across the NE. In general, changes are in general evenly distributed across the region (e.g., end-of-century increases of 9–17% in region 1, 4–16% in region 3). Most increases are projected to occur in the spring and summer for all scenarios and appear to be primarily driven by increasing temperatures and available soil moisture from increased precipitation. Winter evapotranspiration is relatively small in comparison but does show a decrease, especially in the east, because the decrease in snow pack (caused by increased temperatures) reduces the total amount of sublimation.

Increased evapotranspiration combined with low early fall precipitation produces a late summer decrease in soil moisture. These changes are most obvious for A1FI, with its higher temperature change. Winter/early spring soil moisture increases dramatically in the future, driven by more precipitation and increased snowmelt from the higher temperatures.

These changes have important implications for future water availability and drought in the NE. As winters become wetter and summers hotter and drier, agricultural, and natural ecosystems that depend on seasonal rainfall, runoff, and soil moisture are likely to be affected. Any changing balance between evapotranspiration and precipitation during the growing season will have a significant effect on natural vegetation and rainfed agriculture in the region (which includes most crops grown for grain and silage). Changes in vegetation can in turn impact the timing of the hydrological cycle, such as the timing of transition from spring to summer-like conditions (Dirmeyer and Brubaker 2006).

The soil moisture projections presented here, although highly variable, suggest a general increase in dry conditions (Table 3). This is important, as even very short (e.g., 1–4 weeks) water deficits during critical growth stages can have profound effects on plant productivity and reproductive success. These model simulations do not include the changes in seasonal vegetation driven by a longer growing season (i.e., earlier start up and later drop off in transpiration flux); hence, impacts of climate change on summer and fall water availability may be enhanced relative to those projected here. To examine further impacts, we next evaluate potential changes in extreme drought events and general drought frequency across the NE.

4.2 Drought

One of the most important hydrological events in the NE over the past century was the 1960s drought, which

lasted from 1962 to 1965. In addition to the impacts on agriculture and natural ecosystems across the region (Janes and Brumbach 1965; Paulson et al. 1991; Leathers et al. 2000), this drought also greatly reduced water supply. For example, in the summer of 1965, at the height of the drought, New York City stopped releasing water from its Delaware River reservoirs to maintain its withdrawal rate. The resulting drop in Delaware River streamflow levels risked salt-water intrusion into Philadelphia's water supply system (USDA 2000).

With soil moisture, streamflow, and agricultural systems in the NE dependent on natural rainfall, even short periods of drought can have significant impacts. Here, we examine potential changes in two types of drought in the future. The first is a common drought (occurring several times per decade), as defined by VIC-simulated soil moisture deficits, while the second type is severe drought (i.e., similar to the drought observed during the 1960s), and is based on AOGCM-simulated precipitation deficits.

Soil moisture deficits relate directly to the availability of water for agriculture and water supply. They reflect the aggregate effect of all hydrologic processes including changes in short-term precipitation events, temperature swings, evaporative demand, and the longer-term effects of soil drainage and changes in climate (Sheffield et al. 2004b). A climatology of simulated soil moisture values was generated from the VIC retrospective (observationally-driven) simulations. Drought intensity for a particular month was calculated as the percentile soil moisture value relative to the climatology (Sheffield et al. 2004b). A drought event was then specified as a number of consecutive months with soil moisture percentile values less than 10%, with droughts being classified as short- (1–3 months), medium- (3–6 months), and long-term (6+ months).

A general increase in drought frequency is projected in the future, especially under the A1FI scenario (Fig. 6). This is driven by reductions in mean monthly soil moisture during summer and autumn as a result of increased evapotranspiration and reduced precipitation, and is consistent with the projected changes in low-flows discussed next, albeit with changes that are highly variable both spatially as well as between scenarios. Additional increases in evapotranspiration could be expected due to the extension of the growing season. Under the A1FI scenario, the frequency of short-term droughts reaches 1 per year on average in the north and east of the domain by the end of the twenty-first century. Medium-term drought frequencies also increase considerably for A1FI but show only slight changes under B1. Droughts longer than 6 months are infrequent due to the high variability in climate forcings and marked lack of distinct wet/dry seasons, but the local maxima in western New York State increases twofold under A1FI and expands eastward in both scenarios by 2070–2099. This region coincides with the location of maximum drought length, which is over 10 months by 2070–2099.

Due to the importance of the 1960s drought, we also examine model ability to simulate extreme drought events and any potential changes in their return period in the future. The historic drought that persisted throughout the NE in the 1960s was driven primarily by precipitation shortfalls (Namias 1966). We therefore calculate moving averages of precipitation deficits over four, six, eight, and ten consecutive seasons from available USHCN stations and from the historical AOGCM simulations from 1900 to 1999, to quantify precipitation deficits for the most severe drought events over a range of time scales.

Most precipitation-based severe drought events simulated by the AOGCMs for the NE are, on average, less intense than the benchmark 1960s event (Fig. 7). In fact, only two ensemble members—of a total of 38 century-long runs from nine models—simulated an event of greater intensity than observed during the 1960s as measured using any of the four interval periods (four, six, eight, and ten consecutive season intervals). It should be noted, however, that the 1960s event, which peaked during the summers of 1964 and 1965, was the worst drought to occur in the NE region since the beginning of record keeping in the late nineteenth century (Leathers et al. 2000), and possibly since European settlement (Ludlum 1976). Still, we conclude from these results that while the coupled global models are able to simulate meteorologic drought events of moderate persistence, they do not simulate the severe magnitude of precipitation deficits that are comparable to those observed during the 1960s.

The same method was then applied to AOGCM future simulations, where the maximum precipitation shortfalls were computed relative to 1961–1990 averages from each model. Future model projections show greater variation than the historical 20C3M runs (Fig. 7) and the average magnitude of the most severe twenty-first century drought events is projected to be slightly less than twentieth century events, at least in terms of precipitation deficits. However, to account for the fact that the AOGCMs generally project an increase in annual mean precipitation through the twenty-first century (Fig. 2), the same analysis was also conducted on detrended precipitation time series from all B1 and A2 simulations. Not surprisingly, the

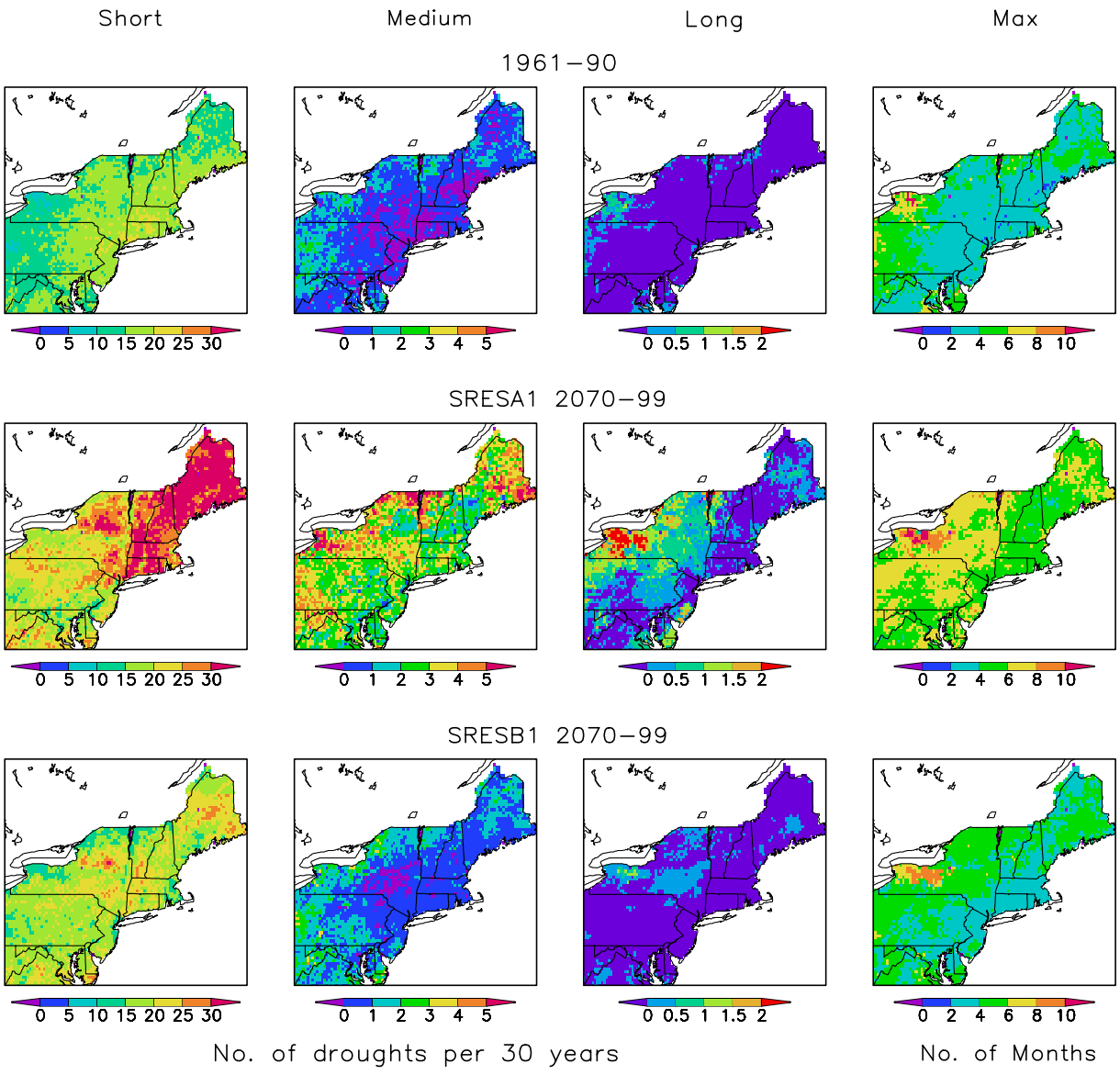

Fig. 6 Frequency of short (1–3 month), medium (3–6 months) and long-term (6 + months) droughts and the maximum drought duration (in months) for the historic (1961–1990) and future (2070–2099) periods. Droughts are defined as deficits of 10% or more in monthly soil moisture relative to the climatological mean. Values are the average of the HadCM3 and PCM-forced VIC simulations for the A1FI and B1 scenarios. Increases are greatest for the shorter drought events and under the A1FI scenario as compared with B1

analysis of detrended output yielded slightly more severe future drought events relative to the raw output, suggesting that our method of characterizing the severity of future drought is somewhat sensitive to projected upward trends in twenty-first century precipitation. Without taking into account projected increases in temperature and evapotranspiration, we conclude from this analysis of AOGCM output alone that severe and persistent region-wide precipitation deficits in the twenty-first century are projected to be roughly equivalent to those observed during the recent past, regardless of the emissions pathway.

Despite the lack of projected changes in extreme precipitation deficits, the projections of drier, hotter summers and more frequent short- and medium-term droughts imply a series of potentially serious impacts on water supply and agriculture. Even very short (1–4 weeks) water deficits during critical growth stages can have profound effects on plant productivity and reproductive success. During a drought, evapotranspiration continues to draw on surface water resources, further depleting supply. As a water deficit deepens, productivity of natural vegetation and agriculture drops. Water use restrictions, such as outdoor watering

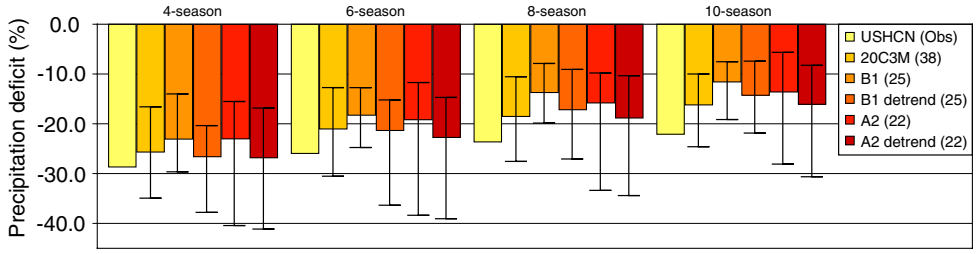

Fig. 7 Mean precipitation deficits (%) corresponding to the most severe observed and simulated drought events in the NE based on moving averages over four, six, eight, and ten consecutive seasons. Results are derived from regionally averaged USHCN station data, historical AOGCM simulations (20C3M; 1900–1999) and twenty-first century climate simulations (B1 and A2; 2000–2099). *Solid bars* indicate the ensemble average value from eight AOGCMs, while the whiskers indicate the range of projections from the full set of models. Numbers in parentheses indicate the number of ensemble members whose results were averaged to generate the displayed values. In general, AOGCM simulations tend to under-estimate the magnitude of potential extreme droughts in the NE, although the uncertainty range encompasses the observed deficits. Little change is projected in the magnitude of future extreme drought events

bans and household conservation measures, are frequently implemented at the city and town level. Increasing water demand has also increased the perceived severity of droughts (Lyon et al. 2005). As soil moisture is further depleted and vegetation becomes increasingly water stressed, the risk of wildfires also rises (e.g., Amiro et al. 2001; Brown et al. 2004).

4.3 Streamflow

We use two metrics to quantify the relationship between climate and streamflow in the NE. The first metric is the *amount* of flow that occurs in specific quantiles, particularly the lowest and highest ones where the greatest impacts can be expected (i.e., floods or dry periods). The second metric is the *timing* of specific events in the annual cycle, such as the timing of high-spring flow and the duration of the low-flow period in the summer.

In general, the AOGCM-driven VIC simulations indicate that climate change is likely to drive a re-distribution of streamflow. There is a general tendency toward more streamflow in winter and spring, and less in summer and fall. This translates into higher winter high-flow events and lower summer low flows. Analysis of projected changes in the probability of winter 10th percentile low flows and 90th percentile high flows (Fig. 8) shows that the probability of winter low flows is likely to decrease by ~5–10% (i.e., more low flow events), with greater changes toward the northern part of the domain. A much larger increase in the probability for high flows is projected, with a greater increase under the A1FI scenario (40–70%) relative to B1 (20–40%) and toward the northern part of the domain where snowmelt is the dominant influence on winter and spring streamflow. An in-depth analysis of projected trends in annual flow quantiles for the single model simulation with the greatest changes (HadCM3 A1FI) for all 51 unmanaged streams from 2000 to 2099 clearly illustrates these opposing trends in different flow regimes (Fig. 9). On an annual basis, from the 50th up to the 95th percentile, there are increases in projected flows, while for the lower 25th down to fifth percentiles, decreases are projected. In other words, these projections indicate increased variability: both more high-flow events and more low-flow events over the course of the year.

The projected increase in variability is consistent with increases in precipitation projected during the late fall, winter, and spring as compared with little to no changes in summer, and with increasing summertime drying due to higher evapotranspiration. Differences between these streamflow projections and earlier ones for the NE that showed decreases in overall streamflow (e.g., Moore et al. 1997) can be attributed to our updated and broader range of AOGCM forcing scenarios, which indicate increases in winter precipitation. Overall, these trends are also consistent with seasonal and annual increases in runoff (Fig. 4) because there are substantially higher flow volumes in the higher (increasing) quantiles than in the lower (decreasing) quantiles.

Increasing trends in late winter and early spring streamflow, and advances of 1–2 weeks in the date of peak streamflow[4] have been observed over the northern part of the NE, with most of the change occurring from 1970 to 2000 (Hodgkins et al. 2003, 2005a). These changes are positively correlated with March–April air temperature, which determines the date at which ice ceases to affect flow[5] as well as the timing of snow melt.

[4] The date of peak streamflow is defined as the center of volume, or the date on which half of the flow occurring between 1 January and 31 May has passed the gauge.

[5] For rivers, the presence of ice can be determined by stream discharge measurements based on continuously measured river stages, which are affected by ice in easily identifiable ways.

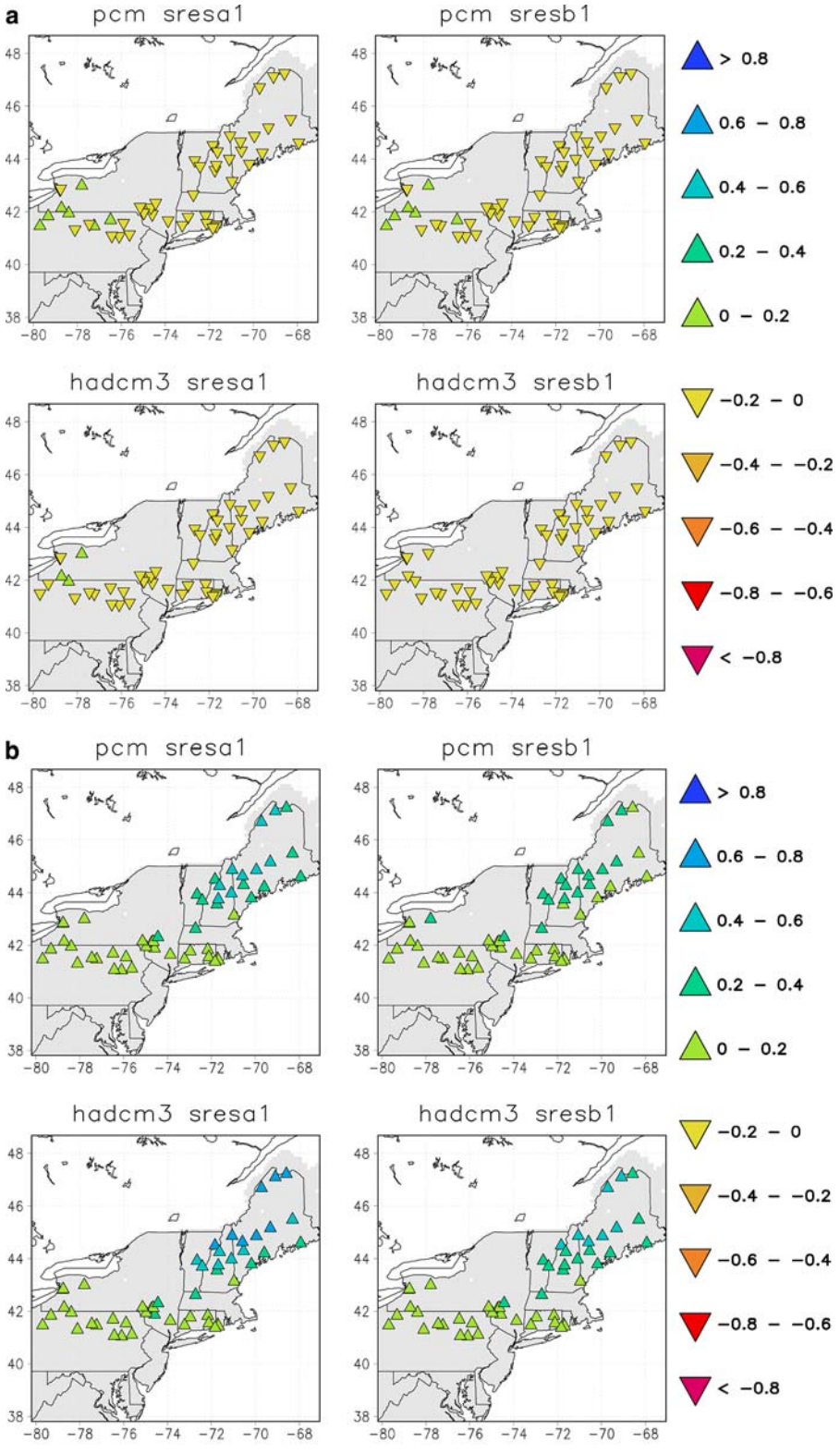

Fig. 8 Projected change in the probability of (**a**) low (10%) and (**b**) high (90%) flows from the historic (1961–1990) to the future (2070–2099) periods for winter (*DJF*) for selected unmanaged basins. AOGCM-driven VIC simulations indicate a decreased probability of low-flow events and increased probability of high flows, with significantly higher flows across much of the northern part of the NE under the A1FI scenario as compared with B1

For example, for 80 stations north of 44°N latitude for the period 1953 through 2002, 69, 75, and 94% of all stations had increasing mean monthly runoff for January, February, and March, respectively (Hodgkins and Dudley 2006b). In contrast, about two-thirds of all stations had trends toward decreasing streamflow for the month of May. Historical records from 1936 to 2000 indicate that, on average, the last dates of

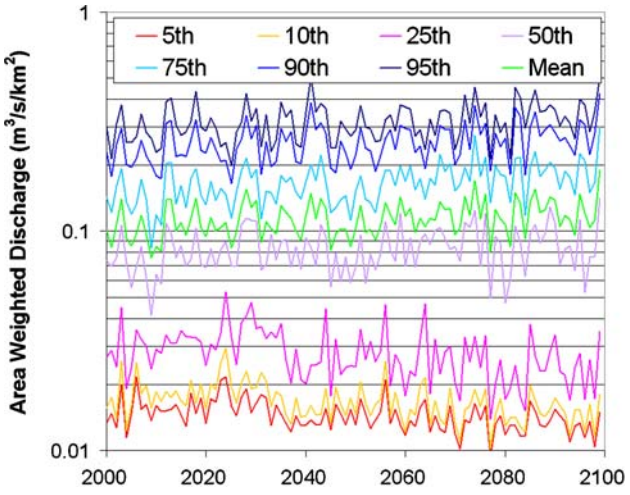

Fig. 9 Twenty-first century stream flow quantiles (in units of m^3/s) based on AOGCM-driven VIC projections for the 51-river area-weighted annual average discharges, calculated based on daily flows from 2000 to 2099. Values shown are based on the HadCM3 climate projections only, for the A1FI scenario. Flows show increasing trends for the 50th quantile and above, and decreasing trends for the 25th quantile and below

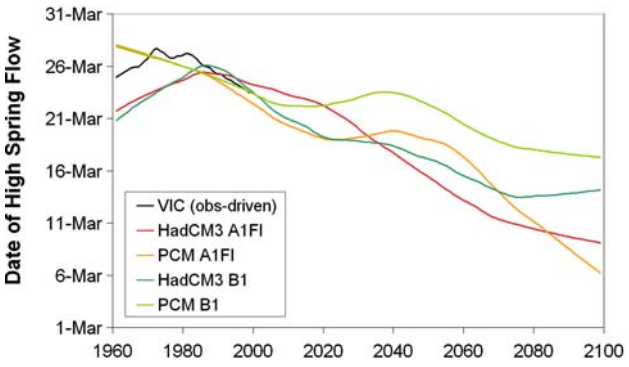

Fig. 10 Projections of timing of snowmelt-driven high spring flow, as represented by shifts in the center of volume date for 51 unregulated rivers in the NE, corresponding to VIC simulations driven by observed temperature and precipitation and by the A1FI and B1 scenarios as simulated by HadCM3 and PCM. By end-of-century, changes under the A1FI scenario are approximately twice those projected under the B1 scenario

ice-affected flow occurred 11 days earlier in the spring in 12 of 16 rural unregulated streams studied (Hodgkins et al. 2005a). These changes are most likely due to shifts in streamflow from later to earlier in the year as snow begins to melt earlier, since late spring streamflow has been decreasing (Hodgkins and Dudley 2006b).

When the VIC model is forced with AOGCM-simulated historical temperature and precipitation from 1960 to 1999, it is able to correctly capture the shift to earlier spring peak flow as measured by stream gauge observations (Fig. 10). However, simulations actually under-estimate the rate of advance (only 0.11 day/year, as compared to the observed average advance of 0.23–0.46 days/year in northern and mountainous areas, Table 2). This is likely due to their failure to capture the dramatic winter warming the NE has experienced over that time. This trend also may reflect the shift toward an increase in the ratio of rain to snow in the winter (Huntington et al. 2004).

In the future, peak streamflow in spring is projected to continue to occur earlier in the year, with further advances of 5–8 days by mid-century (Fig. 10). End-of-century changes are larger under the higher emissions scenario (+15 days under A1FI as compared to +10 days under B1).

In the summer and autumn, streamflow tends to drop as temperatures and evaporation rise. The US Fish and Wildlife Service (USFWS) has defined a low flow threshold of 0.5 cfs/sq mi ($0.037\ m^3/s/km^2$), equivalent to August median flow, as the minimum streamflow required for summertime maintenance of habitat for biota in New England streams (USFWS 1981). The flow in many streams currently drops below this threshold for several weeks in mid- to late-summer, but more frequent and/or extended periods of streamflow below this threshold could adversely affect stream habitat for aquatic biota.

During the twentieth century, no significant decrease in summer/fall low flows or change in the timing of those low-flow events has been observed (Hodgkins et al. 2005b). Increases in precipitation over the last century may have compensated for any increases in evapotranspiration, masking any underlying trend.

Projected future changes in low-flow amounts and duration differ significantly between the higher A1FI and lower B1 scenarios. Under A1FI, the 7-day consecutive low-flow amounts from every year are projected to decrease on the order of 10% or more for 51 unmanaged rivers in the NE (Fig. 11). Changes under B1 are smaller, <10% for HadCM3 and little net change for PCM. In terms of the length of the USFWS low-flow threshold, projections for the A1FI indicate that by end-of-century most streams will drop below this threshold about 3 weeks earlier in the year, and delay their return above this threshold by about 3 weeks in the fall, while little changes are estimated for B1 (Fig. 12). However, even under the B1 scenario, streamflow remains significantly below the historical mean during early to mid fall. This suggests that even with the projected increases in precipitation over the winter months, we should anticipate some considerable impacts related to more extensive low-flow periods during summer months, particularly under a higher

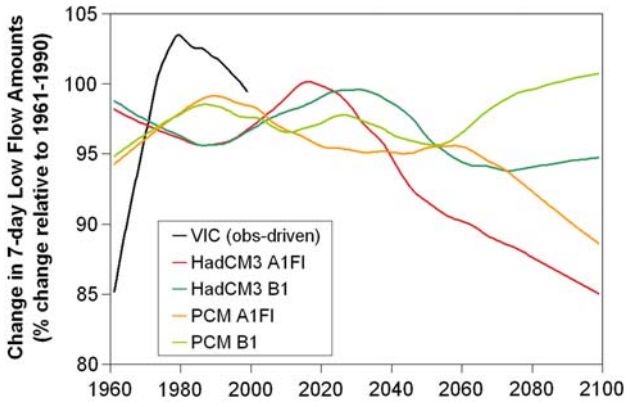

Fig. 11 Projections of the change in the lowest consecutive cumulative 7-day flow amounts for each year for 51 unregulated rivers in the NE corresponding to corresponding to VIC simulations driven by observed temperature and precipitation and by the A1FI and B1 scenarios as simulated by HadCM3 and PCM. Values are shown relative to the 1961–1990 average (100%), although historical curves fall below this value due to the LOWESS smoothing function, which minimizes the influence of outliers and in that sense is more analagous to the median than the mean (Helsel and Hirsh 1992). Observation-driven VIC simulations show the influence of the extraordinary 1960s drought. In the future, A1FI scenarios show decreasing trends in the average low-flow amounts, while B1-based changes are ambiguous

emission scenario. Furthermore, it appears that these changes likely represent the net effect of interactions between multiple factors, with the effect of temperature-driven increases in evapotranspiration beginning to dominate under the higher A1FI scenario.

These projections indicate more variability in flow, with significant implications for many aspects of the NE. Overall, the impacts are likely to be greatest for aquatic biota most sensitive to the timing of high-spring flow (such as spring spawners), and for river systems where even moderate reductions in summer low flows could adversely affect habitat or place added pressure on competition for surface water resources. Higher winter flows are related to an increase in the frequency of mid-winter ice jams that resulted in major flooding and damage to infrastructure (Beltaos and Prowse 2002). Changes in the timing of high-spring flow may also influence survival of Atlantic salmon. If spring peak migration of juvenile salmon from freshwater rivers (which is controlled by a combination of photoperiod, temperature, and flow) becomes out of phase by as much as 2 weeks with optimal environmental conditions in rivers, estuaries or the ocean, salmon survival could be adversely affected (McCormick et al. 1998). Another concern is rising water temperatures (e.g., the Wild River in Maine, Huntington et al. 2003). Ecological projections call for major stress on cold-water fish in the next century due to rising temperatures alone (e.g., Schindler 2001). These changes will likely be exacerbated by the low-flows projected to occur under higher emission scenarios. Finally, even in NE where water is considered relatively abundant, there are already issues arising over competition for limited water supplies among agricultural (e.g., blueberries in Maine), industrial

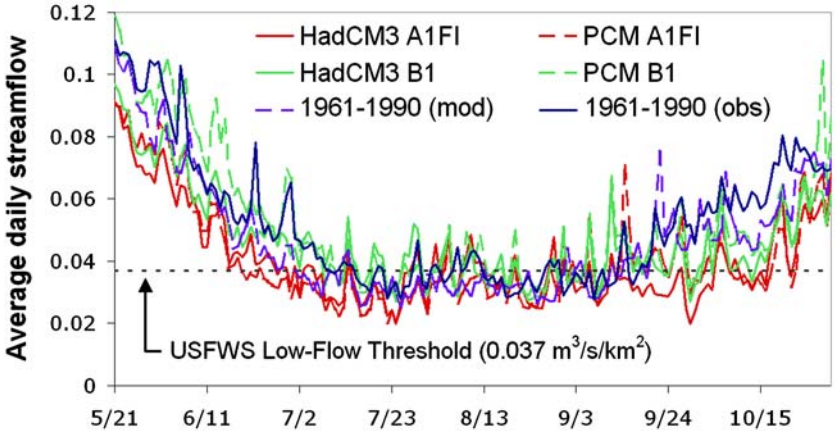

Fig. 12 Projected changes in average daily flows during the period 21 May through 31 October, in units of cubic meters per second per square kilometer of drainage area, such that the overall average reflects the mean of the 51 stream values irrespective of the area of their drainage basins. 1961–1990 (*mod*) is based on VIC-simulated hydrology driven by HadCM3/PCM simulations based on estimated natural and human forcing, while 1961–1990 (*obs*) is based on VIC-simulated hydrology driven by observed temperature and precipitation over that time. Future projections correspond to VIC model simulations driven by the A1FI and B1 scenarios as simulated by HadCM3 and PCM. The US Fish and Wildlife Service (*USFWS*) low flow threshold of 0.037 $m^3/s/km^2$ (USFWS 1981) is shown for reference. Compared with the *black line* (historical observations), the scenarios tend to drop below the threshold earlier and remain below it longer by ~3 weeks under the A1FI scenarios and a few days to a week under B1

(hydropower generation), municipal, recreational, and ecological/habitat concerns. These will likely be exacerbated by the imposition of additional variability and shifts in streamflow timing due to the climate change over the coming century documented here.

4.4 Snowfall and snow cover

Another hydrological indicator often used to characterize the NE is the extent and duration of snow cover. Although winters in the NE are generally snowy, over the last few decades more winter precipitation has falling as rain and less as snow, particularly at the more northern sites (Huntington et al. 2004). Here, we examine trends in the amount of snow on the ground (as measured by snow density or SWE), the total number of snow-covered days in winter, and the overall length of the snow season.

As the snow data from snow course sites is limited (for example, there are only 23 locations in Maine and only a few of these have records that extend back into the early part of the last century), we again combine observations with analysis of the retrospective or observation-driven VIC simulations. For the period 1950–1999, observationally driven VIC simulations show snow water equivalence (SWE) across the NE decreasing by 0.03 mm/decade while AOGCM-driven VIC simulations show SWE increasing by 0.05 mm/decade. The number of snow days decreases at a rate of –0.04 and –0.07 days/month/decade based on the observed- and AOGCM-driven VIC simulations, respectively. These trends are consistent with observed

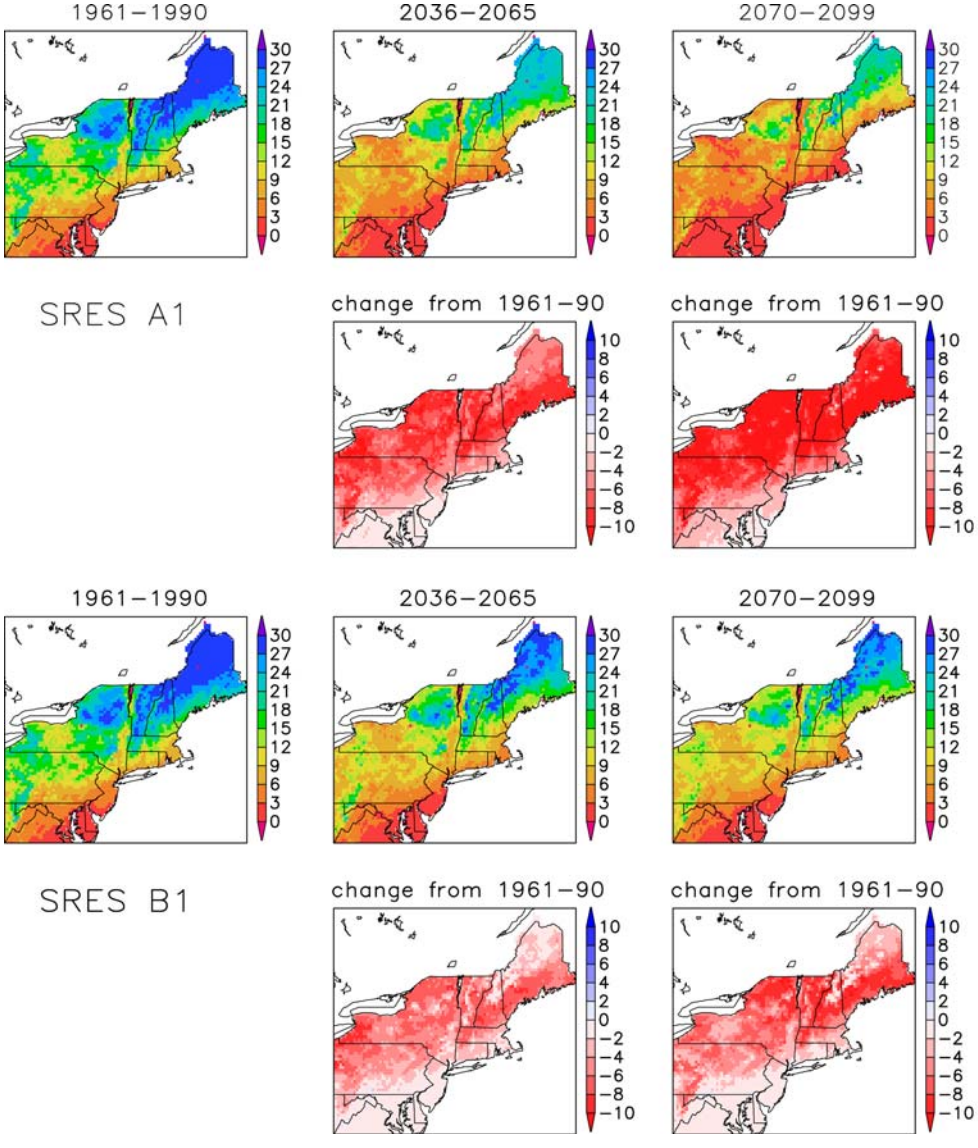

Fig. 13 Number of snow-covered days per month for winter (*DJF*) averaged over 30-year historic and future periods. Also shown are the differences in number of snow-covered days between the future and historic period. Values are the average of the HadCM3 and PCM-forced VIC simulations

trends of decreasing snow cover but increasing density (Huntington et al. 2004; Hodgkins and Dudley 2006a). During the last 30 years of the period (1970–1999), decreasing trends in SWE (–3.52 and –2.9 mm/decade from observed- and AOGCM-driven runs) and snow days (–0.5 and –0.6 days/month/decade from observed- and AOGCM-driven runs) are significant at the 95% level, and are likely due to the increasing temperatures coupled with a decreasing snow-to-total precipitation ratio.

A snow-covered day is defined as one with mean SWE greater than an arbitrary threshold value of 5 mm. Snow cover is generally restricted to the winter months, mostly in the north and higher elevations. The number of snow-covered winter (DJF) days in the historic period (1961–1990) ranges from close to zero day/month south of Pennsylvania to 30 days/month in parts of northern New York, Vermont, New Hampshire and Maine. In the future, model-driven VIC simulations show a general decrease in the number of snow days, most notably across the central part of the domain and southern Maine (Fig. 13). These decreases occur mainly at the edge of the snowline where the threshold between snow and no snow is most sensitive. Decreases are greatest for the higher-temperature A1FI scenario relative to B1 (Table 3), and are primarily driven by increasing temperatures, especially in February and March. These reduce the number of freezing days and thus the ratio of snowfall to rainfall events, as well as increasing the likelihood of warm rain falling on existing snowpack and accelerating the snowmelt. Warm temperatures can also cause existing snow to melt more rapidly.

Interestingly, in the southern part of the domain under the B1 scenario and in the northeastern part of the region in late spring under other scenarios, little change in the number of snow days is seen by 2070–2099. This is likely due to the relatively smaller increase in temperature being offset by a larger increase in precipitation. In other words, in the southern part of the NE, there are relatively few days when it is cold enough to snow there already. So, although the projected warming in winter temperature will still decrease the number of cold days, the projected increase in precipitation means that the chances that it could actually snow on more of those days could increase even if there are fewer days. In terms of snow days in late spring, it is likely that increased precipitation is compensating for increased snowmelt from the higher temperatures.

In the future, the winter snow season is shortened in all regions, with snow appearing later in the winter and disappearing earlier in the spring. This is most evident in northern regions where snow is more prevalent. Both scenarios show large reductions in the length of the snow season in winter/early spring with greater than 50 and 25% reductions in the number of snow days by 2070–2099 under scenarios A1FI and B1, respectively.

These changes have the potential to affect the NE in several ways. First, we have already hypothesized that the rapid winter warming observed over recent decades may be related to snow-albedo feedbacks on a regional scale that are not accurately captured by global models. Additional snow loss may serve to further enhance winter warming over the next few decades, particularly over the northern part of the domain. Economic sectors affected by snow loss include the ski and snowmobile industries that depend on winter snow cover for recreational opportunities and related revenue (e.g., Hamilton et al. 2003). Snow loss would also affect forests and natural ecosystems that rely on winter snow cover for protection during frosts and as a source of soil moisture in spring (Perfect et al. 1987). A reduction in snow-cover days in winter would increase the frequency of freeze-thaw cycles, which research has shown affects winter soil microbial processes such that nitrogen losses as nitrate leaching and gaseous flux of nitrous oxide are increased (Brooks 1998; Groffman et al. 2001; Dorsh 2004). Increased frequency of freeze-thaw cycles also leads to increased root damage (Perfect et al. 1987).

5 Biometeorological indicators

A third type of climate indicator is that which reflects changes in biologically-relevant temperature thresholds. Temperature thresholds determine the response of flora, fauna, and agriculture in the NE to climate change. Biological activity is often sensitive to temperature thresholds and to a build-up of temperature over days and months, creating unique cumulative rather than instantaneous indicators. Here, we examine freeze dates and the length of the growing season (determined by temperature thresholds), and the SI (determined by the accumulated days of winter chilling and the spring warming), indicative of the onset of vegetation growth in the spring.

5.1 Growing season and freeze dates

Historically across the US, the length of the winter freeze period has already been decreasing over the last half of the past century (Kunkel et al. 2004; Schwartz et al. 2006). Multi-model simulations suggest that the

number of frost days is expected to continue to decline in the future across the entire Northern Hemisphere, while the growing season will expand (Tebaldi et al. 2006).

Here, we define the growing season as being the length of time between the last spring freeze of the year and the first hard freeze of the following autumn where daily minimum temperatures drop to or below –2.2°C (28°F), after Schwartz et al. (2006). In the NE, the growing season typically lasts for about half the year, or 185 days. Over the period of record (1915–2003), the length of the growing or frost-free season has been increasing at an average of +0.7 days/decade. Over the last 30 years (1970–2000), the observed trend based on daily station data across the NE has increased to +2.4 days/decade. While first freeze dates in autumn are occurring somewhat later, the observed increase in growing season length is being driven primarily by earlier last freeze dates in spring (Schwartz et al. 2006). It is uncertain whether this phenomenon is responding to late winter snow-albedo feedbacks, whereby more rapid melting of snow in spring (as seen in the advance of peak spring streamflow) could be preventing late-season freezes, or whether it is a simple function of a greater rate of spring temperature increases as compared with autumn (although the fact that the models also simulate a greater change in spring freeze dates but do not reproduce a greater change in winter temperatures as compared with other seasons suggests that this may not be the primary mechanism). By mid-century, enough warming is projected to have occurred such that the ''easy'' freezes just below the temperature threshold in late winter and early spring will not occur. Thus, the growing season will be lengthened by eliminating the much colder days that occur during the winter months from freezing—a more difficult task.

In the future, the multi-model ensemble average suggests that by mid-century (here defined as 2045–2064 due to the limited daily temperature output available for all but the HadCM3, PCM, and GFDL models) the growing season may be 2–4 weeks longer than during the 1961–1990 reference period. By end-of-century (2080–2099), the growing season may be extended by an average of 4 weeks under the lower B1 scenario and 6 weeks under the higher A1FI and A2 scenarios. For relatively small temperature changes (B1 mid-century), model simulations suggest that the retreat of spring freeze dates continues to be the primary cause of the lengthening growing season, as observed over the past few decades. On average, under B1 the mid-century spring last freeze is coming 9 days earlier and the autumn first freeze only 0.6 days later. However, for B1 end-of-century and under A1FI/A2, projections suggest that the process causing spring changes to be the dominant driver of growing season change saturates. Instead, projected changes in last freeze are almost equivalent to the projected changes in first freeze, with both contributing nearly equally to the expanding growing season for temperature changes in excess of ~2°C.

5.2 Spring indices

The second set of indicators examined here are the SI. These consist of SI first leaf date, an ''early spring'' average date among the three indicator plants related to a general onset of growth in grasses and shrubs, and SI first bloom date, a ''late spring'' average date when flowers in three indicator species start to open, related to a general onset of growth in dominant forest vegetation. The first leaf date is particularly important from an ecological perspective as it often displays the strongest response to temperature change, and is crucial for accurate assessment of processes related to the start and duration of the growing season (Schwartz et al. 2006).

An advance of –2.10 days/decade in SI first leaf date has been previously documented over the NE from 1960 to 2000, along with an advance in SI first bloom date of –1.23 days/decade, based on daily temperature records from 68 co-op stations, with both trends significant at $P < 0.001$ (Wolfe et al. 2005). Using observed station temperature records in the NE from 1916 to 2003, SI first leaf date and first bloom date showed moderate advancement (both –0.4 days/decade). Over the last few decades (1970–2000), however, both begin to advance at accelerated rates of –2.2 and –0.9 days/decade (Table 2; again, all trends significant at the 0.001 level). AOGCM-driven SI simulations from 1916 to 2000 also show a decreasing trend toward earlier in the year, although with a tendency to underestimate the rate of change (Table 2)—again, perhaps related to the large winter temperature increases that have been observed but are not reproduced by the AOGCM simulations (Fig. 14). The model ensemble average trends from 1970 to 2000 are –1.4 and –0.7 days/decade for SI first leaf and first bloom dates, respectively (Table 2)—again, slightly less than observed trends during that period. During recent decades, all models displayed a late bias (averaging 6 days with a range from 2 to 9 days depending on the model), with GFDL being the best predictor of mean SI first leaf and first bloom date.

Examining future projected changes in the SI dates for the three AOGCMs with continuous daily temperature projections available over the next century,

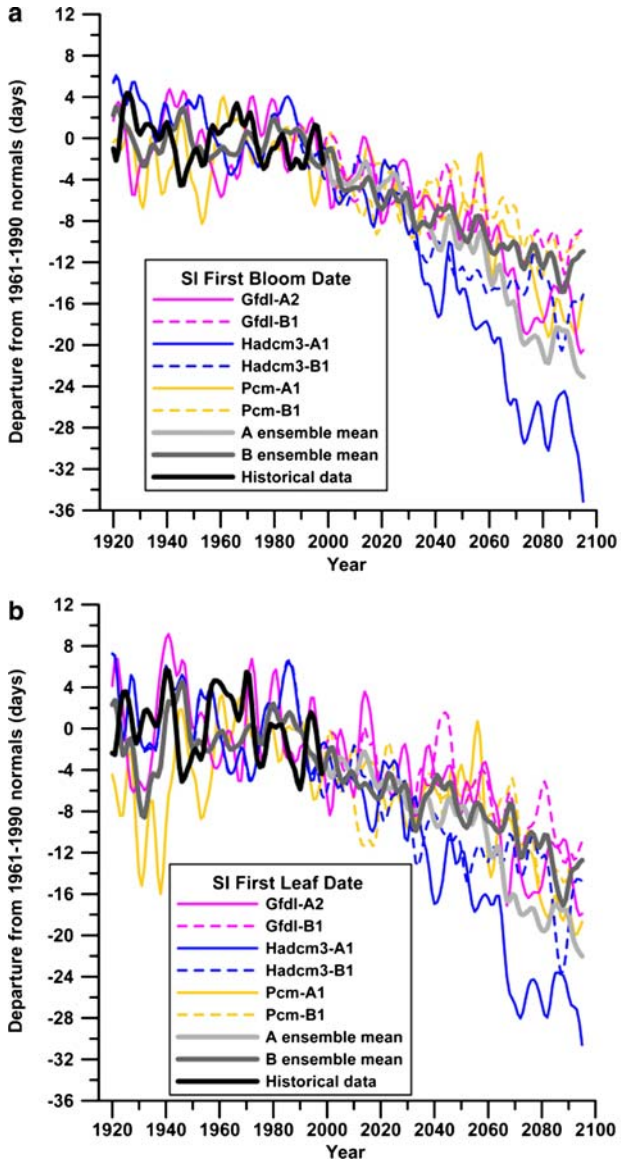

Fig. 14 Spring Indices (*SI*) first leaf date departures (**a**) and first bloom date departures (**b**) by scenario (in days) over the 1916–2099 period (each line smoothed by a nine-point normal-curve filter). Both historical data and model output show a trend toward earlier dates which, by end-of-century, becomes more pronounced under the higher A1FI and A2 scenarios (*solid lines*) relative to B1 (*dashed lines*)

we see a consistent trend toward earlier dates, with changes of –2.1 and –2.3 days/decade or almost 3 weeks earlier by end-of-century under A1FI/A2 and –1.0 and –0.9 days/decade or 1–2 weeks earlier by end-of-century under B1 for SI first leaf and first bloom dates, respectively (Fig. 14). Additional simulations based on four AOGCMs for which daily output were only available for the time periods 2046–2065 and 2081–2099 were also consistent with these findings, with A1FI/A2 scenarios suggesting that average SI first leaf dates will become ~5 days and SI first bloom dates ~6 days earlier in 2047–2065, and an additional 10 days earlier by 2082–2099 (compared to the observed values during 1961–1990 and considering the previously mentioned late biases, Table 3). Under B1, the changes are only slightly less by mid-century (~3 days for SI first leaf date and 4 days for SI first bloom date), but considerably smaller than A1FI/A2 by end-of-century (only 2–4 additional days earlier, Table 3). This model is expected to be robust under conditions where climate departs significantly from the historical mean, as the SI models are optimized for continental-scale applications and included input data from a study area that extended southward from the US NE to North Carolina, and then westward to Oklahoma and North Dakota (Schwartz 1997). Thus, SI model results for future warming in the NE are well within the range of actual phenological values and temperatures used in model development and testing.

5.3 Implications for natural and managed ecosystem response

Projected changes in the timing of the growing season and the onset of spring, combined with rising temperatures, shifts in streamflow, increased frequency of summer droughts, and other changes examined here will have impacts on both natural and managed systems. Some animals, plants, insects, and pathogens will benefit, while others do poorly, for a number of reasons.

First, a warming climate is likely to exacerbate problems associated with invasive species (Weltzin et al. 2003), and will alter important interactions and synchrony between plants and pollinators, insect pests, diseases, and weeds (Walther 2002). The current historical trend showing more warming in winter than in other seasons of the year could have numerous ecological consequences, such as more overwintering of insect pests, and insufficient duration of winter cold to fully meet vernalization requirements of some plant species, which negatively affects spring flowering.

The projected increase in the frequency of high day and night temperatures in spring and summer will negatively affect flowering, fruit set, and/or seed production of many plant species, including high-value horticultural crops (Peet and Wolfe 2000). Even a warm-season adapted crop such as tomato can have reduced yield and/or quality if temperatures exceed 32°C for short periods during critical flowering and pollination periods (Sato et al. 2001).

A general warming trend will clearly lengthen the growing season and result in early flowering for many

plant species, as already observed and as predicted here by the SI model (Wolfe et al. 2005; Fig. 14). In addition, it will hasten plant development throughout the summer, increasing pressure on water resources in the region and altering the timing of the hydrological cycle (Dirmeyer and Brubaker, 2006). Warmer summers can reduce yield of many important grain crops, such as maize, wheat, and oats, due to a shortening of the grain-filling period (e.g., Mitchell et al. 1993). Farmers in the region can adapt to climate change by shifts in varieties or crop species, but suitable options may not always be available, adaptation costs may be high, or there may be market constraints to the introduction of new varieties or new crops.

6 Conclusions

Temperatures across the US Northeast have been warming steadily since the 1970s. A wide range of indicators in the NE have already been observed to be responding to these changes, which in turn have the potential to impact urban and rural life, agriculture, industry, tourism, and natural ecosystems.

Combining past observed trends with AOGCM simulations of future climate enables us to paint a coherent picture of the types of physical and biological changes that might be expected across the region over the coming century. Focal areas studied here include changes in the distribution of seasonal temperature and precipitation; their impact on evaporation, runoff, and soil moisture characteristics of the region; resulting shifts in stream flow amounts and distribution over the year; impacts on drought characteristics and snow cover; and finally, implications of temperature change for cultivated and natural plant species via the length of the growing season and SI calculations. Although the mechanisms responsible for determining the net changes in each of these are complex, most display a consistent signal in response to warming temperatures.

Historical model simulations that include the influence of human emissions on climate are able to reproduce the sign of observed trends in most temperature-related climate indices (including mean annual and seasonal temperatures, snow cover and extent, streamflow, and SI). This suggests that AOGCMs are capable of reproducing the dominant influence on regional temperature-related climate indicators. However, model simulations fail to capture the regional effects leading to strong observed winter warming, and generally tend to *underestimate* the magnitude of observed trends, particularly over the last few decades. This implies that regional processes may be acting to enhance warming trends in the NE relative to the global average in a way not captured by global-scale models.

Over the coming century, temperature increases are projected to be significantly greater under a higher as compared to a lower emissions scenario, with equal or greater increases in summer relative to winter. Winter precipitation is likely to increase by 10–15%, consistent with recent observed trends, while summer precipitation shows either little change or a decrease. These conclusions regarding inter-scenario and seasonal differences are consistent across the 23 future simulations from the nine AOGCMs examined here (CCSM3, CGCM3, CSIRO, ECHAM5, GISS-E-R, GFDL2.1, HadCM3, Miroc, and PCM). Additional changes in snow depth and extent, timing of streamflow, growing season, SI, and other temperature-related climate indices all show trends that are consistent with warming temperatures, with significantly larger trends under the higher SRES emissions scenarios (A1FI, A2) as compared to a lower scenario (B1). Even indicators that might be expected to depend more strongly on precipitation rather than on temperature show strong trends, such as earlier spring melt dates and prolonged summer low-flow periods, which can likely be explained by increased evaporation due to warmer temperatures that is not balanced by an increase in summer precipitation.

Some differences in climate projections still remain to be resolved, particularly those related to the fine-scale spatial and temporal distribution of changes over a geographically diverse region such as the US NE. However, the model-simulated trends in temperature and precipitation-related indicators examined here are reasonably consistent with both observed historical trends as well as a broad range of future model simulations. These suggest confidence in the direction and potential range of regional trends in these indicators, which clearly depends on the emissions pathway we follow over the next century.

Acknowledgments This manuscript benefited greatly from comments and suggestions by Dan Cayan and Chester Zenone (USGS), and two anonymous reviewers. We acknowledge the international modeling groups for providing their data for analysis, the Program for Climate Model Diagnosis and Intercomparison (PCMDI) for collecting and archiving the model output, the JSC/CLIVAR Working Group on Coupled Modeling (WGCM) and their Coupled Model Intercomparison Project (CMIP) and Climate Simulation Panel for organizing the model output analysis activity, and the IPCC WG1 TSU for technical support. The IPCC Data Archive at Lawrence Livermore National Laboratory is supported by the Office of Science, US Department of Energy. We gratefully acknowledge the Union of Concerned Scientists, who catalyzed this research as the first stage of a forthcoming Northeast Climate Impacts Assessment

Report. Contributions to this study were as follows: synthesis and manuscript preparation, model-simulated temperature and precipitation analysis, growing season analysis, data provision for hydrological and biometerological analyses (Hayhoe), synthesis and manuscript preparation, observed temperature and precipitation analysis (Wake), observed and model-simulated streamflow analysis (Huntington), VIC and river routing model simulations (Luo), SI and growing season analysis (Schwartz), VIC data analysis for terrestrial hydrology, streamflow, drought and snow (Sheffield), hydrologic analysis and support (Wood), precipitation and temperature extremes and synthesis (Anderson), SST and drought analysis (Bradbury), precipitation and temperature extremes (DeGaetano), assistance with VIC model simulations (Troy), ecosystem response analysis (Wolfe).

References

Abdulla FA, Lettenmaier DP, Wood EF, Smith JA (1996) Application of a macroscale hydrologic model to estimate the water balance of the Arkansas-Red river basin. J Geophys Res 101(D3):7449–7459

Amiro BD, Stocks BJ, Alexander ME, Flannigan MD, Wotton BM (2001) Fire, climate change, carbon and fuel management in the Canadian boreal forest. Int J Wildland Fire 10:405–413

Beltaos S, Prowse TD (2002) Effects of climate on mid-winter ice jams. Hydrol Proc 16:789–804

Bradbury JA, Dingman SL, Keim BD (2002) New England drought and relations with large scale atmospheric circulation patterns. JAWRA 38:1287–1299

Brooks PD (1998) Inorganic nitrogen and microbial biomass dynamics before and during spring snowmelt. Biogeochemistry 43:1–15

Brown TJ, Hall BL, Westerling AL (2004) The impact of twenty-first century climate change on wildland fire danger in the western United States: an applications perspective. Clim Change 62:365–388

Cherkauer KA, Bowling LC, Lettenmaier DP (2002) Variable Infiltration Capacity (VIC) cold land process model updates. Glob Planet Change 38:151–159

Collins WD, Bitz CM, Blackmon ML, Bonan GB, Bretherton CS, Carton JA, Chang P, Doney SC, Hack JJ, Henderson TB, Kiehl JT, Large WG, McKenna DS, Santer BD, Smith RD (2006) The Community Climate System Model: CCSM3. J Clim 19:2122–2143

Dai A, Hu A, Meehl GA, Washington WM, Strand WG (2004) Atlantic thermohaline circulation in a coupled general circulation model: unforced variations versus forced changes. J Clim 18:3270–3293

Daly C, Taylor G, Gibson W (1997) The PRISM approach to mapping precipitation and temperature. In: Tenth conference on applied climatology. American Meteorological Society, Reno, NV, pp10–12

DeGaetano AT, Allen RJ (2002) Trends in twentieth-century temperature extremes across the United States. J Clim 15:3188–3205

Delworth TL, Broccoli AJ, Rosati A, Stouffer RJ et al (2006) GFDL's CM2 global coupled climate models—Part 1—formulation and simulation characteristics. J Clim 19:643–674

Diffenbaugh NS, Pal JS, Trapp RJ, Giorgi F (2005) Fine-scale processes regulate the response of extreme events to global climate change. PNAS 102:15774–15778

Dirmeyer PA, Brubaker KL (2006) Evidence for trends in the northern hemisphere water cycle. Geophys Res Lett 33:L14712. DOI 10.1029/2006GL026359

Dorsch P (2004) Overwintering greenhouse gas fluxes in two contrasting agricultural habitats. Nutr Cycling Agroecosyst 70:117–133

Easterling DR, Karl TR, Lawrimore JH, Del Greco SA (1999) United States historical climatology network daily temperature, precipitation, and snow data for 1871–1997. ORNL/CDIAC-118, NDP-070. Carbon Dioxide Information Analysis Center, Oak Ridge National Laboratory, US Department of Energy, Oak Ridge, TN

Gibbs JP, Breisch AR (2001) Climate warming and calling phenology of frogs near Ithaca, NY, 1900–1999. Conserv Biol 15:1175–1178

Gordon HB, Rotstayn LD, McGregor JL, Dix MR, Kowalczyk EA, O'Farrell SP, Waterman LJ, Hirst AC, Wilson SG, Collier MA, Watterson IG, Elliott TI (2002) The CSIRO Mk3 Climate System Model (Electronic publication). Aspendale: CSIRO Atmospheric Research (CSIRO Atmospheric Research technical paper; no. 60), 130pp. Available on-line at: http://www.dar.csiro.au/publications/gordon_2002a.pdf

Groffman PM, Driscoll CT, Fahey TJ, Hardy JP, Fitzhugh RD, Tierney GL (2001) Effects of mild winter freezing on soil N and C dynamics in a northern hardwood forest. Biogeochemistry 56:191–213

Guttman N, Quayle R (1996) A historical perspective of US climate divisions. Bull Am Met Soc 77:293–303

Hamilton LC, Rohall D, Brown B, Hayward G, Keim B (2003) Warming winters and New Hampshire's lost ski areas: an integrated case study. Int J Soc Soc Policy 23:52–73

Hamlet AF, Lettenmaier DP (2005) Production of temporally consistent gridded precipitation and temperature fields for the continental United States. J Hydrometeorol 6:330–336

Hasumi H, Emori S (eds) (2004) K-1 coupled model (MIROC) description, K-1 technical report 1. Center for Climate System Research, University of Tokyo, 34pp. Available at: http://www.ccsr.u-tokyo.ac.jp/kyosei/hasumi/MIROC/tech-repo.pdf

Hayhoe K, Cayan D, Field CB, Frumhoff PC, Maurer EP, Miller NL, Moser SC, Schneider SH, Nicholas Cahill K, Cleland EE, Dale L, Drapek R, Hanemann RM, Kalkstein LS, Lenihan J, Lunch CK, Neilson RP, Sheridan SC, Verville JH (2004) Emissions pathways, climate change, and impacts on California. Proc Natl Acad Sci 101:12422–12427

Helsel DR, Hirsch RM (1992) Statistical methods in water resources, studies in environmental science, vol 49. Elsevier, New York, 522 p

Hodgkins GA, James IC, Huntington TG (2002) Historical changes in lake ice-out dates as indicators of climate change in New England, 1850–2000. Int J Climatol 22:1819–1827

Hodgkins GA, Dudley RW, Huntington TG (2003) Changes in the timing of high river flows in New England over the 20th century. J Hydrol 278:244–252

Hodgkins GA, Dudley RW, Huntington TG (2005a) Changes in the number and timing of ice-affected flow days on New England rivers, 1930–2000. Clim Change 71:319–340

Hodgkins GA, Dudley RW, Huntington TG (2005b) Summer low flows in Northeast over the 20th century. Am Water Resour Assoc J 41:403–412

Hodgkins GA, Dudley RW (2006a) Changes in late-winter snowpack depth, water equivalent, and density in Maine, 1926–2004. Hydrol Process 20:741–751

Hodgkins GA, Dudley RW (2006b) Changes in the timing of winter-spring high streamflows in eastern North America 1912–2002. Geophys Res Lett 33 DOI 10.1029/2005GL025593

Huntington TG, Hodgkins GA, Dudley RW (2003) Historical trend in river ice thickness and coherence in hydroclimatological trends in Maine. Clim Change 61:217–236

Huntington TG, Hodgkins GA, Keim BD, Dudley RW (2004) Changes in the proportion of precipitation occurring as snow in Northeast (1949 to 2000). J Clim 17:2626–2636

Huntington TG (2006) Evidence for intensification of the global water cycle: review and synthesis. J Hydrol 319:83–95

Janes BE, Brumbach JJ (1965) The 1964 agricultural drought in connecticut. University of Connecticut Agricultural Experiment Station Bulletin 390, Storrs, 22p

Juanes F, Gephard S, Beland KF (2004) Long-term changes in migration timing of adult Atlantic salmon (Salmo salar) a the southern edge of the species distribution. Cdn J Fish Aquatic Sci 61:2392–2400

Karl TR et al (1986) A model to estimate the time of observation bias with monthly mean maximum, minimum, and mean temperatures for the United States. J Clim Appl Meteorol 25:145–160

Karl TR, Williams CN Jr (1987) An approach to adjusting climatological time series for discontinuous inhomogeneities. J Clim Appl Meteorol 26:1744–1763

Karl TR, Diaz HF, Kukla G (1988) Urbanization: its detection and effect in the United States climate record. J Clim 1:1099–1123

Karl TR, Williams CN Jr, Quinlan FT, Boden TA (1990) United States Historical Climatology Network (HCN) Serial Temperature and Precipitation Data, Environmental Science Division, Publication No. 3404. Carbon Dioxide Information and Analysis Center, Oak Ridge National Laboratory, Oak Ridge, TN, 389 pp

Keim BD, Wilson A, Wake C, Huntington TG (2003) Are there spurious temperature trends in the United States Climate Division Database? Geophys Res Lett 30(27):1404, DOI 10.1029/2002GL016295

Keim BD, Fischer MR, Wilson AM (2005) Are there spurious precipitation trends in the United States Climate Division database? Geophys Res Lett 32:L04702, DOI 10.1029/2004GL021985

Kim S-J, Flato GM, Boer GJ, McFarlane NA (2002) A coupled climate model simulation of the Last Glacial Maximum, Part 1: transient multi-decadal response. Clim Dyn 19:515–537

Kim S-J, Flato GM, Boer GJ (2003) A coupled climate model simulation of the Last Glacial Maximum, Part 2: approach to equilibrium. Clim Dyn 20:635–661

Kunkel KE, Easterling DR, Hubbard K, Redmond K (2004) Temporal variations in frost-free season in the United States: 1895–2000. Geophys Res Lett 31:L03201. DOI 10.1029/2003GL018624

Kushnir Y, Robinson WA, Blade I, Hall NMJ, Peng S, Sutton R (2002) Atmospheric GCM response to extratropical SST anomalies: synthesis and evaluation. J Clim 15:2233–2256

Leathers DJ, Grundstein AJ, Ellis AW (2000) Growing season moisture deficits across the northeastern United States. Clim Res 14:43–55

Liang X, Lettenmaier DP, Wood EF, Burges SJ (1994) A simple hydrologically based model of land surface water and energy fluxes for GSMs. J Geophys Res 99(D7):14,415–14,428

Liang X, Wood EF, Lettenmaier DP (1996) Surface soil moisture parameterization of the VIC-2L model: evaluation and modifications. Glob Planet Change 13:195–206

Ludlum DM (1976) The Country Journal: Northeast Weather Book. Houghton Mifflin, Boston

Lyon B, Christie-Blick N, Gluzberg Y (2005) Water shortages, development, and drought in Rockland County, New York. Am Water Resour Assn J 41:1457–1469

Maurer EP, O'Donnell GM, Lettenmaier DP, Roads JO (2001) Evaluation of the land surface water budget in NCEP/NCAR and NCEP/DOE reanalyses using an off-line hydrologic model. J Geophys Res 106:17841–17862

Maurer EP, Wood AW, Adam JC, Lettenmaier DP, Nijssen B (2002), A long-term hydrologically-based data set of land surface fluxes and states for the conterminous United States. J Clim 15:3237–3251

McCormick SD, Hansen LP, Quinn TP, Saunders RL (1998) Movement, migration, and smolting of Atlantic salmon (Salmo salar). Cdn J Fish Aquatic Sci 55:77–92

Mitchell RAC, Mitchell VJ, Driscoll S et al (1993) Effects of increased CO2 concentration and temperature on growth and yield of winter wheat at two levels of nitrogen application. Plant, Cell Environ 16:521–529

Moore MV, Pace ML, Mather JR, Murdoch PS, Howarth RW, Folt CL, Chen CY, Hemond HF, Flebbe PA, Driscoll C (1997) Potential effects of climate change on freshwater ecosystems of the New England/Mid-Atlantic region. Hydrol Process 11:925–947

Nakićenović N et al (2000) IPCC special report on emissions scenarios. Cambridge University Press, Cambridge, UK and New York, NY

Namias J (1966) Nature and possible causes of the northeastern United States Drought during 1962–1965. Mon Weather Rev 94(9):543–557

Nijssen B, O'Donnell GM, Lettenmaier DP, Lohmann D, Wood EF (2001) Predicting the discharge of global rivers. J Clim 14:3307–3323

Paulson RW, Chase EB, Roberts RS, Moody DW (1991) National water summary 1988–1989: hydrologic events and floods and droughts. US Geological Survey Water Supply Paper No. 2375, Denver Co., 591p

Peet MM, Wolfe DW (2000) Crop ecosystem responses to climate change—vegetable crops. In: Reddy KR, Hodges HF (eds) Climate change and global crop productivity. CABI Publishing, New York

Perfect E, Miller RD, Burton B (1987) Root morphology and vigor effects on winter heaving of established alfalfa. Agron J 79:1061–1067

Pope VD, Gallani ML, Rowntree PR, Stratton RA (2000) The impact of new physical parameterizations in the Hadley Centre climate model—HadCM3. Clim Dyn 16:123–146

Primack D, Imbres C, Primack RB, Miller-Rushing A, del Tredici P (2004) Herbarium specimens demonstrate earlier flowering times in response to warming in Boston. Am J Bot 91(8):1260–1264

Quayle RG, Easterling DR, Karl TR, Hughes PY (1991) Effects of recent thermometer changes in the cooperative station network. Bull Am Meteorol Soc 72:1718–1724

Roeckner E, Bäuml G, Bonaventura L, Brokopf R, Esch M, Giorgetta M, Hagemann S, Kirchner I, Kornblueh L, Manzini E, Rhodin A, Schlese U, Schulzweida U, Tompkins A (2003) The atmospheric general circulation model ECHAM5. Part I: model description. Max Planck Institute for Meteorology Rep. 349, 127pp. Available from MPI for Meteorology, Bundesstr. 53, 20146 Hamburg, Germany

Sato S, Peet MM, Gardener RG (2001) Formation of parthenocarpic fruit and aborted flowers in tomato under moderately elevated temperatures. Sci Hortic 90:243–254

Schindler DW (2001) The cumulative effects of climate warming and other human stresses on Canadian freshwaters in the new millennium. Can J Fish Aquat Sci 58:18–29

Schmidt GA et al (2006) Present day atmospheric simulations using GISS ModelE: comparison to in-situ, satellite and reanalysis data. J Clim 19:153–192

Schwartz MD (1997) Spring index models: an approach to connecting satellite and surface phenology. In: Lieth H, Schwartz MD (eds) Phenology in seasonal climates I. Backhuys, Leiden, pp 23–38

Schwartz MD, Ahas R, Aasa A (2006) Onset of spring starting earlier across the Northern hemisphere. Glob Change Biol 12:343–351

Schwartz MD, Reiter BE (2000) Changes in North American Spring. Int J Climatol 20:929–932

Sheffield J, Ziegler AD, Wood EF, Chen Y (2004a) Correction of the high-latitude rain day anomaly in the NCEP/NCAR reanalysis for land surface hydrological modeling. J Clim 17(19):3814–3828

Sheffield J, Goteti G, Wen F, Wood EF (2004b) A simulated soil moisture based drought analysis for the United States. J Geophys Res 109, D24108, DOI 10.1029/2004JD005182

Smith TM, Reynolds RW (2003) Extended reconstruction of global Sea surface temperatures based on COADS Data (1854–1997). J Clim 16:1495–1510

Tebaldi C, Hayhoe K, Arblaster J, Meehl G (2006) Going to the extremes: an intercomparison of model simulated historical and future changes in extreme events. Clim Change (in press)

Trombulak SC, Wolfson R (2004) Twentieth-century climate change in Northeast and New York, USA. Geophys Res Lett 31 DOI 10.1029/2004GL020574

US Department of Agriculture (2000) Preparing for drought in the 21st Century. National drought policy commission report, http://www.fsa.usda.gov/drought/finalreport/fullreport/ndpcfullreportcovers/ndpcreportsummaryv.htm

US Fish and Wildlife Service (1981) Interim regional policy for New England stream flow recommendations: region I. US Fish and Wildlife Service, Concord, NH, 3pp

VanRheenan NT, Wood AW, Palmer RN, Lettenmaier DP (2004) Potential implications of PCM climate change scenarios for Sacramento-San Joaquin River Basin hydrology and water resources. Clim Change 62:257–281

Wake CP, Markham A (2005) Indicators of climate change in the Northeast 2005. Clean Air-Cool Planet, Portsmouth, NH. Available on-line at: http://www.cleanair-coolplanet.org

Walther GR (2002) Ecological responses to recent climate change. Nature 416:389–395

Washington WM et al (2000) Parallel Climate Model (PCM) Control and transient simulations. Clim Dyn 16:755–774

Wehner MF (2004) Predicted twenty-first-century changes in seasonal extreme precipitation events in the parallel climate model. J Clim 17:4281–4290

Weltzin JF, Travis-Belote R, Sanders NJ (2003) Biological invaders in a greenhouse world: will elevated CO_2 fuel plant invasions? Front Ecol Environ 1(3):146–153

Williams CN Jr, Menne MJ, Vose RS, Easterling DR (2005) United states historical climatology network monthly temperature and precipitation Data.ORNL/CDIAC-118, NDP-019. Available on-line at: http://cdiac.ornl.gov/epubs/ndp/ushcn/usa_monthly.html from the Carbon Dioxide Information Analysis Center, Oak Ridge National Laboratory, US Department of Energy, Oak Ridge, TN

Wolfe DW, Schwartz MD, Lakso A, Otsuki Y, Pool R, Shaulis N (2005) Climate change and shifts in spring phenology of three horticultural woody perennials in northeastern USA. Int J Biometeor 49:303–309

Wood AW, Maurer EP, Kumar A, Lettenmaier DP (2002) Long-range experimental hydrologic forecasting for the eastern United States. J Geophys Res 107:Art. No. 4429

Wood A, Leung LR, Sridhar V, Lettenmaier D (2004) Hydrologic implications of dynamical and statistical approaches to downscaling climate model surface temperature and precipitation fields. Clim Change 62:189–216